Science of the Total Environment 951 (2024) 175257

Contents lists available at ScienceDirect

Science of the Total Environment

journal homepage: www.elsevier.com/locate/scitotenv

Modelling alternative harvest effects on soil CO_2 and CH_4 fluxes from peatland forests

Xuefei Li [a,*], Tiina Markkanen [b], Mika Korkiakoski [b], Annalea Lohila [a,b], Antti Leppänen [a], Tuula Aalto [b], Mikko Peltoniemi [c], Raisa Mäkipää [c], Thomas Kleinen [d], Maarit Raivonen [a]

[a] Institute for Atmospheric and Earth System Research (INAR)/Physics, Faculty of Science, University of Helsinki, P.O. Box 68, 00014 Helsinki, Finland
[b] Finnish Meteorological Institute, P.O. Box 503, 00101 Helsinki, Finland
[c] Natural Resources Institute Finland, Helsinki, Finland
[d] Max Planck Institute for Meteorology, Bundesstr.53, 20146 Hamburg, Germany

HIGHLIGHTS

- Harvest effects on soil GHG from peatland forest were successfully simulated.
- Model showed tradeoff between soil CH4 & CO2 via harvest-induced water table change.
- Selection harvesting is bigger soil C source than clear-cut when recently harvested.

GRAPHICAL ABSTRACT

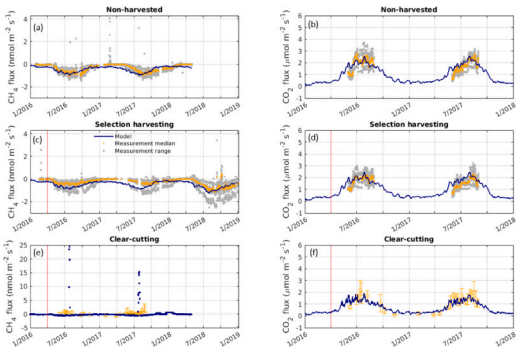

ARTICLE INFO

Editor: Martin Drews

Keywords:
Peatland forest
Alternative harvesting regimes
Modelling
Soil CH_4 flux
Soil respiration
Water level

ABSTRACT

Over the last century, many peatlands in northern Europe have been drained for forestry. Forest management with different harvesting regimes has a significant impact on soil water status and consequently on greenhouse gas emissions from peat soils. In this paper, we have used the process-based JSBACH-HIMMELI model to simulate the effects of alternative harvesting regimes, namely non-harvested (NH), selection harvesting (SH; 70 % of stem volume harvested) and clear-cutting (CC; 100 % of stem volume harvested), on soil CH_4 and CO_2 fluxes in peatland forests. We modified the model to account for the specific characteristics of peatland forests, where the water level (WL) is generally low and is regulated by the amount of aboveground vegetation through evapotranspiration. Multi-year measurements before and after the forest harvesting in a nutrient-rich peatland forest in southern Finland were used to constrain the model.

The results showed that the modified model was able to reproduce the seasonal dynamics of water level, soil CH_4 and soil CO_2 fluxes under alternative harvesting regimes with reasonable accuracy. The averaged *Pearson's r* (Pearson correlation coefficient) and *RMSE* (Root Mean Square Error) between the model and the measurement were 0.75 and 7.3 cm for WL, 0.75 and 0.23 nmol m^{-2} s^{-1} for soil CH_4 flux, 0.73 and 0. 88 μmol m^{-2} s^{-1} for soil

* Corresponding author.
E-mail address: xuefei.z.li@helsinki.fi (X. Li).

https://doi.org/10.1016/j.scitotenv.2024.175257
Received 15 December 2023; Received in revised form 21 June 2024; Accepted 1 August 2024
Available online 8 August 2024

CO_2 flux. The modified model successfully reproduced soil CH_4 uptake at both NH and SH sites and soil CH_4 emission at the CC site, as observed in the measurements.

Our study showed that increasing harvesting intensity (NH → SH → CC) in the model increased soil CH_4 emission and decreased soil CO_2 emission on an annual basis, but the magnitude of the decreased soil CO_2 emission was much larger than that of the increased soil CH_4 emission when comparing their global warming potentials. Therefore, in the short term as in our study (first three years after the harvest), the climate impacts of the soil GHG was reduced more in CC than in SH, which yet can be fundamentally different when considering in the long term.

1. Introduction

Peatlands, a significant terrestrial carbon reservoir, cover approximately 3 % of the global land surface, but contain about one-third of the world's total soil organic carbon (SOC) pool due to the very low decomposition rate under anoxic soil conditions (Yu, 2011; Nichols and Peteet, 2019). In recent decades, 150,000 km^2 of pristine peatlands have been drained for forestry in the boreal and temperate regions to increase tree growth (Paavilainen and Päivänen, 1995). In Finland alone, more than half of the original 100,000 km^2 of peatlands have been drained for forestry (Päivänen and Hånell, 2012; Turunen, 2008). The amount of SOC stored in peatland forest soils at the European scale has been estimated to be 578 t C ha^{-1} within 1 m depth from the surface, about five times higher than that stored in mineral soils (De Vos et al., 2015).

When peatland forests reach the end of their rotation cycle, they are harvested for commercial purposes. There are two main forest management practices: even-aged management (EM) and continuous cover forestry (CCF). One of the main differences between these practices is the harvesting method. EM involves clear-cutting (CC) of forests followed by soil preparation, maintenance of the ditch network and planting or seeding. CCF, on the other hand, never clears the forest, but rather partially harvests it, leaving a proportion of tree stand on the site after harvesting and damaging less ground vegetation. Although EM is currently the dominant management practice currently, CCF has gained increasing attention as an alternative management option to EM due to its potential environmental benefits, especially in peatland forests (Nieminen et al., 2018).

The different harvesting intensities applied in EM and CCF could lead to substantial changes in the environmental conditions of the peatland forests, affecting the soil greenhouse gas (GHG) balance of these forests (Mayer et al., 2020; Mäkipää et al., 2023). In the CC of EM, tree removal leads to a rise in the water level (WL; positive value means above peat surface) due to reduced transpiration and interception of precipitation (Sarkkola et al., 2010). The raised WL can decrease soil respiration due to the reduced aeration in the soil (Minkkinen and Laine, 1998; Ojanen et al., 2013) while it can increase CH_4 emission or decrease CH_4 oxidation by reducing the thickness of the oxic peat layer in the soil (Lai, 2009; Peltoniemi et al., 2023). It also dramatically changes the microclimate by increasing the amount of solar radiation reaching the forest floor (Korkiakoski et al., 2020), changing wind flow patterns, decreasing net radiation and increasing albedo (Mamkin et al., 2019). In contrast, the selective harvesting applied in CCF could keep the WL low through the remaining trees and other vegetation on the site (Leppä et al., 2020). The lower WL results in lower CH_4 emissions but higher soil CO_2 emissions (Ojanen and Minkkinen, 2019).

In order to estimate the climatic impacts of different harvesting intensities in wider temporal and spatial scales, process-based modelling is needed. The use of process-based models to simulate the effects of alternative harvesting methods on soil GHGs in peatland forests has so far been scarce. Kasimir et al. (2018) used the Coup model (Jansson, 2012) to simulate GHG emissions from a Norway spruce peatland forest with different WLs and plant species, but they did not compare the effects of different harvesting options. Shanin et al. (2021) simulated the effects of different harvest intensities on GHG emissions from nutrient-rich peatland forests. However, in their study the CO_2 and CH_4 fluxes from the peat layer were calculated using empirical equations, i.e., not process-based. There are several process-based peatland models that simulate the vertical biogeochemistry in the soil, including CH_4 and oxygen concentrations, and are capable of simulating both CH_4 uptake and CH_4 emissions (Kaiser et al., 2017; Riley et al., 2011). However, we did not find studies in which they were applied specifically for CH_4 uptake or the trade-off between CO_2 and CH_4, nor comparisons between time series of modelled and observed CH_4 uptake fluxes. On the other hand, models developed for simulating CH_4 uptake by mineral soils (Curry, 2007; Murguia-Flores et al., 2018) do not include the possibility for CH_4 emission and are not designed for peat soils.

To fill this gap, we modified and applied HelsinkI Model of MEthane buiLd-up and emIssion for peatlands (HIMMELI; Raivonen et al., 2017) to simulate soil CO_2 and CH_4 fluxes from peatland forests under alternative harvesting regimes. We utilized Jena Scheme for Biosphere-Atmosphere Coupling in Hamburg (JSBACH; Reick et al., 2021) to provide the hydrological and carbon inputs for HIMMELI. The JSBACH-HIMMELI model framework was constrained with measured data from Lettosuo in Southern Finland, where different sections received different harvesting options, namely clear-cutting (CC), selection harvesting (SH) and non-harvested (NH). The aim of the study was to develop a version of the JSBACH-HIMMELI model that can simulate the impact of different harvesting on soil CO_2 and CH_4 exchange in a peatland forest.

JSBACH has previously been applied to boreal forest (e.g. Mäkelä et al., 2019) and pristine peatland (Kleinen et al., 2020), and the JSBACH-HIMMELI combination to pristine peatland (Petrescu et al., 2023), but not to drained peatland forest. In contrast to pristine peatland where WL remains high and large amounts of CH_4 are often emitted, the WL in peatland forest is usually low and both CH_4 uptake and emission can be observed from the forest floor. In addition, there is higher decomposition of peat in peatland forests (i.e., CO_2 flux from the forest floor) due to the higher oxygen levels in the peat. Considering these features, we hypothesize that with simple modifications, the JSBACH-HIMMELI model framework can be used to simulate (1) the variation in water level caused by alternative harvesting practices, (2) both CH_4 uptake and CH_4 emission as a function of harvesting practices, and (3) a trade-off between soil CH_4 and CO_2 emission from peatland forests that varies with different harvesting practices.

2. Materials and methods

2.1. Model description and development

2.1.1. JSBACH model

JSBACH is a process-based ecosystem model, which is the land surface component of the Max Planck Institute Earth System Model [MPI-ESM] (Reick et al., 2021). JSBACH was originally used for global simulations, but was later also been applied to boreal forest ecosystems at the site scale (Böttcher et al., 2016; Mäkelä et al., 2019). In JSBACH, the land surface is divided into grid cells, which are classified as bare soil or vegetated area, and the vegetated area is further divided into tiles. The site in our study was represented as a single grid point with full vegetation coverage for all tiles, i.e., there was no bare soil. The current version of JSBACH has a multilayer soil hydrological scheme with increasing layer thickness. The lower boundary is at 4.3 m. The general

model description e.g. surface processes, water balance, heat transfer, etc., can be found in Reick et al. (2021). In the following sections we will focus on the processes that have been modified for the simulation of peatland forests.

2.1.1.1. Photosynthesis and phenology. In JSBACH, photosynthesis was described by the Farquhar model (Farquhar et al., 1980) and the process was realized in two steps. In the first step, the photosynthetic productivity of the canopy was resolved in an unstressed condition. This potential productivity determined the potential stomatal conductance, which was used to calculate the potential water loss by transpiration. In the second step, limiting water supply had a scaling effect on the potential stomatal conductance so that it was reduced to the actual stomatal conductance, which was then used in the photosynthesis routine to produce the actual productivity (Reick et al., 2021). The parameters were adopted from the default values from JSBACH model code. The maximum carboxylation rate ($V_{C,\ max}$) at 25 °C was 62.5 μmol (CO_2) m^{-2} s^{-1} and the maximum electron transport rate (J_{max}) at 25 °C was 118.8 μmol (CO_2) m^{-2} s^{-1}.

Photosynthesis was constrained by the leaf area index (LAI), which follows a phenological cycle. LAI (m^2 m^{-2}) is a measure of the total one-sided leaf area projected onto a given land area. The Logistic Growth Phenology (LoGro-P) module in JSBACH was used to predict the seasonal variation of vegetation phenology (Böttcher et al., 2016). In this module, the LAI of each plant functional type (PFT) was determined by air temperature, soil moisture and maximum LAI (LAI_{max}), a key parameter describing a physiological limit of the vegetation. As LAI_{max} reflects the leaf growth capacity of the site, we used it as a proxy for the vegetation status in our simulations. Specifically, we adjusted the LAI_{max} values for each post-harvest year to account for the harvesting practice used on the site and the recovery of vegetation after the harvest. Site-level net ecosystem exchange (NEE) and gross primary production (GPP) measurements were used to constrain the LAI_{max} values (see Section 2.5.1).

Although the JSBACH model allowed fractional coverage of several PFTs, we adopted coniferous evergreens as the only vegetation type represented on the grid cell. The photosynthetically active period has been found to be too early for coniferous evergreens in a previous study (Böttcher et al., 2016). This is because evergreens do not shed all their leaves in winter, allowing them to quickly resume photosynthesis in the following spring. In order to limit the too early start of the photosynthetically active period in the model, we adopted the modification for a delayed effect of temperature on photosynthesis as presented in Mäkelä et al. (2019), and we further defined this modification to be effective only in spring.

2.1.1.2. Soil carbon model. For the decomposition of soil organic matter (SOM), JSBACH uses the soil carbon module YASSO (Goll et al., 2015; Tuomi et al., 2009). YASSO consists of four carbon pools, representing carbon fractions that are soluble in water (W), in the non-polar solvent ethanol (E), hydrolysable in acid (A), as well as a fraction that is neither soluble nor hydrolysable (N). These pools are replicated for leaf and woody litter and for above and below ground. The belowground also contains a fifth carbon pool, the humus pool, which contains SOM that has undergone substantial decomposition. Each pool has its own mass loss rate from the system and mass flow rate between pools due to the decomposition of the compound.

Similar to most other soil carbon models, the basic YASSO does not consider the specific conditions of peatlands, i.e., the dependence of soil carbon decomposition on the WL and oxygen conditions, including the strong decrease in decomposition rate in the permanently anoxic catotelm. In our study, we used the YASSO modified for peatlands ($YASSO_{peatland}$), which extends the basic YASSO to peatlands with two main modifications (Petrescu et al., 2023). First, WL was included in the simulation of soil decomposition. Anaerobic decomposition was allowed to happen in the fraction of the soil column below the current WL, and the decomposition rates in this part were reduced by a modification factor of 0.35 for pristine peatlands, following Wania et al. (2010). Second, the humus carbon pool was removed from the carbon pools and replaced by a catotelm carbon pool containing the carbon in the lower part of the soil column. In this part, the decomposition rate was further reduced by a factor of 0.125 to achieve a decomposition rate constant of 7.0×10^{-5} yr^{-1}, similar in magnitude to Kleinen et al. (2012) and Clymo et al. (1998). Catotelm height was determined from the basic YASSO humus pool size. Acrotelm area was defined as the top of the litter layer. Acrotelm height was determined from YASSO aboveground and belowground carbon pool sizes. Specifically for drained peatlands, we increased the acrotelm decomposition by a factor of 1.25 because decomposition rates in well-drained soils are typically rapid due to the increased oxygen levels in the surface layers of drained peatlands (Moore and Basiliko, 2006). The relative mass flow magnitude between the different carbon pools were also adjusted. A list of key parameters that have been modified in the $YASSO_{peatland}$ is shown in Table S1.

2.1.1.3. Soil hydrology. In the $YASSO_{peatland}$, WL was controlled by the equilibrium evapotranspiration (Petrescu et al., 2023). Here we used an approach where WL followed soil moisture, which was affected by simulated transpiration. Therefore, in our approach, WL is directly related to the amount of aboveground transpiring vegetation:

$$WL = n + \left(\frac{W_s}{\theta_{FC} \times Z_r} - 1\right) \times m \quad (1)$$

where W_s was the total soil moisture in the rooting zone (m), θ_{FC} was the field capacity (m/m), Z_r was the rooting depth (m), m and n were the scaling parameters (discuss below). θ_{FC} and Z_r had constant values in all simulations (Table S1). $\theta_{FC} \times Z_r$ showed the maximum soil moisture in the rooting zone, so $\frac{W_s}{\theta_{FC} \times Z_r}$ was always <1. We introduced the scaling parameters n to adjust the overall level (positive value raises the WL) and m to adjust the range of the simulated WL, as preliminary tests showed too little variation of simulated WL compared to observations when WL was modelled based on soil moisture alone.

As WL is directly affected by the evapotranspiration strength of the forest stand (Leppä et al., 2020), m and n were defined as a function of LAI_{max} ($LAI_{max} > 0$). In particular, we used 2-parameter asymptotic exponential equations to describe the relationships between m or n and LAI_{max}, as the effects should level out with increasing stand volume (Sarkkola et al., 2010):

$$m = a_1\left(1 - e^{-b_1 \times LAI_{max}}\right) \quad (2)$$

$$n = a_2\left(1 - e^{-b_2 \times LAI_{max}}\right) \quad (3)$$

where a_1, b_1 and a_2, b_2 are tuning parameters. (1)–(3) were fitted to the measured WL during the post-harvest period and the LAI_{max} from each site using the least-squares approach (function "nlinfit" from Matlab). LAI_{max} values from the first year after harvest were used in the fitting (LAI_{max} = 1, 2.5 and 3.5 for CC, SH and NH sites, respectively). The optimized values for $a_1 = 2.086$, $b_1 = 1.131$, $a_2 = 0.383$ and $b_2 = 0.942$. The fitted models and observed values are shown in Fig. S1.

Model sensitivity tests showed that the parameterization of m and n had the largest effects on the WL simulation at the lowest LAI_{max}, i.e., reduced tree cover, and the effects decreased with increasing LAI_{max} (Fig. 1 a–c). Sensitivity tests also showed the increasing trends in anaerobic respiration (R_{anae}) with decreasing LAI_{max} (Fig. 1d). Prominent R_{anae} were simulated when WL was within the acrotelm (on average the simulated boundaries between acrotelm and catotelm varied between −0.16 and −0.18 m). When WL varied within the catotelm, R_{anae} did not respond much to the changes in WL.

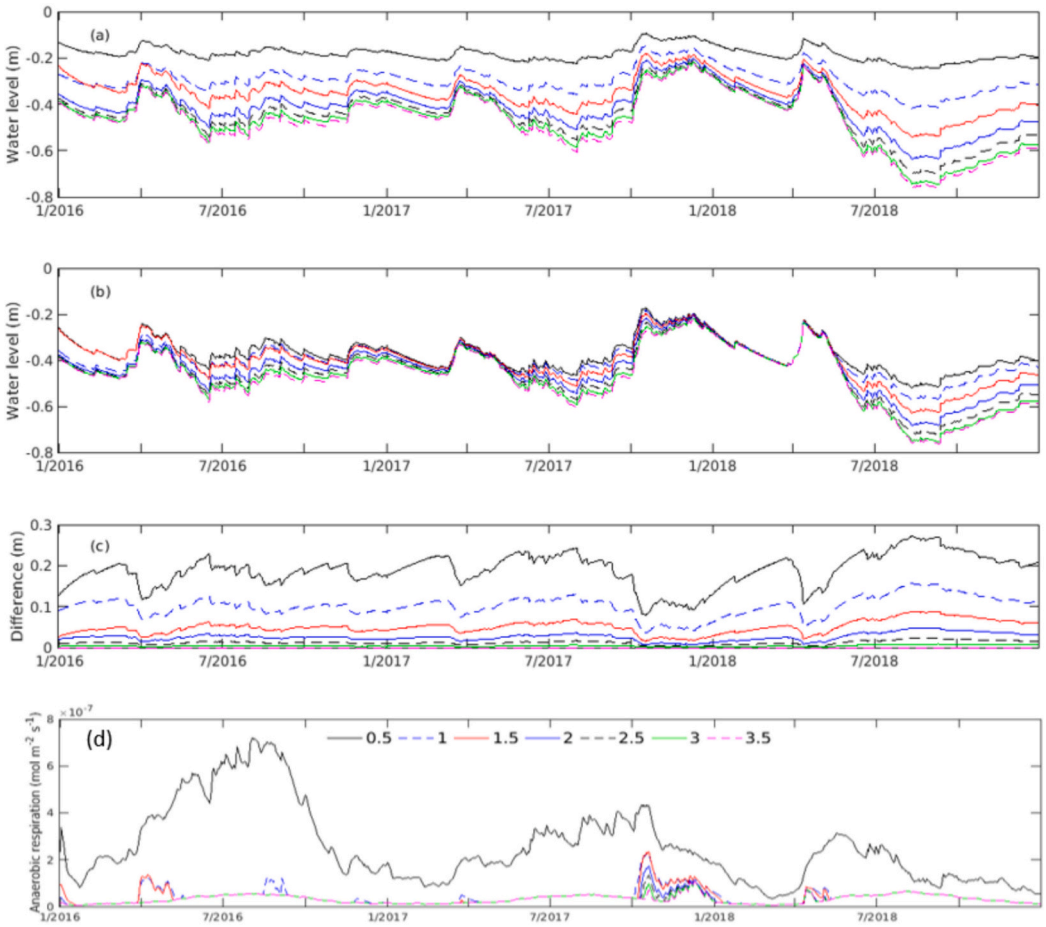

Fig. 1. Simulated water level during the post-harvest years 2016–2018 with (a) adjusted and (b) constant parameters *m* and *n* when different LAI_{max} values (0.5, 1, 1.5, 2, 2.5, 3 and 3.5) were given. In (a), *m* and *n* were simulated separately with Eqs. (2) and (3) at each LAI_{max}. In (b), the constant parameters *m* and *n* fitted when $LAI_{max} = 3.5$ were applied for all the simulations. (c) showed the difference between (a) and (b). (d) showed model sensitivity test of anoxic respiration, where *m* and *n* varied in each simulation as in (a).

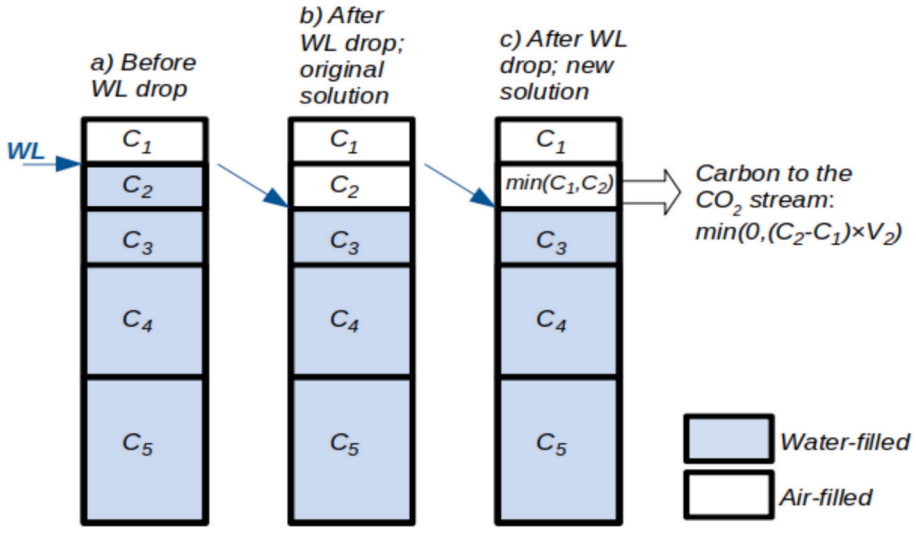

Fig. 2. An illustration of the modified treatment of concentrations in the case of dropping water level (WL) in HIMMELI. The gridded vertical boxes represent the modelled peat column divided into five layers that are either water-filled (below WL) or air-filled (above WL). C_1-C_5 indicate concentrations (CH_4, CO_2 or O_2) in each of the five layers. a) Before WL drop, C_1 is concentration in the topmost air-filled peat layer and C_2-C_5 are concentrations of dissolved gas in water-filled layers. b) In the original HIMMELI, WL drop does not affect the concentration (C_2) in the newly air-filled peat layer. c) In the modified version of HIMMELI, the newly air-filled peat layer has either the same concentration than before WL drop (C2) or concentration of the air-filled layer above it (C_1), depending on which of them is smaller. In the cases of CO_2 and CH_4, if C1 is smaller, the difference is added to the CO_2 emission stream. If C1 was smaller in the case of O_2, the excess O_2 is just lost – but this is not expected to happen as dissolved O_2 concentrations are lower than in the air-filled peat.

2.1.2. HIMMELI v200

HIMMELI is a process-based CH_4 model that simulates the processes related to the build-up of CH_4, CO_2 and O_2 in the soil, the transport of compounds and the oxidation of CH_4 (Raivonen et al., 2017). HIMMELI is driven by soil temperature, WL, anaerobic carbon decomposition rate and LAI of aerenchymatous gas-transporting vegetation. HIMMELI considers the net balance among several microbial processes and transport pathways of CH_4, CO_2 and O_2 dynamics in a one-dimensional, vertically layered peat column: CH_4 production, aerobic respiration, CH_4 oxidation, ebullition, diffusion in the peat (air and water) and gas transport in the plant aerenchyma. The outputs of the model are fluxes of CH_4, CO_2 and O_2 between the soil and the atmosphere, and the pathways (ebullition, diffusion and plant-transport) of the output CH_4 and CO_2 fluxes are specified. Our starting point was HIMMELI v1.0.1, i.e., the published code with a few bug fixes.

HIMMELI v1.0.1 has so far been applied to pristine peatlands that were net sources of CH_4. Preliminary tests on Lettosuo, a drained peatland, confirmed that the model could correctly simulate downward CH_4 flux (uptake) when CH_4 production was low and there was a sufficient aerobic peat layer above the WL (data not shown). However, in HIMMELI v1.0.1, the masses of different compounds (O_2, CH_4, and CO_2) were conserved over WL drops by introducing the compounds dissolved in water into the new air-filled peat layer (Fig. 2a and b). In the case of CH_4, it is immediately released into the atmosphere by diffusion due to the concentration gradient, which has created artificial CH_4 emission peaks when WL drops. In the pristine peatlands, the magnitude of the maximum CH_4 emissions in summer could reach about 100 nmol m^{-2} s^{-1} and the variation in WL was modest (Raivonen et al., 2017; Rinne et al., 2018). Under these conditions, emission peaks caused by changing WL were a small fraction of the total flux. However, in the peatland forest, where WL remained significantly below the peat surface (on average −40 cm before harvest) and there was a low CH_4 uptake of the order of 1 nmol m^{-2} s^{-1}, these peaks were prominent (Fig. S2). In our modification, the new air-filled layer was assigned the same gas concentration as either the previously water-filled layer or the air-filled layer above it, depending on which was smaller (Fig. 2c). In the case of CH_4, the excess of CH_4 (the difference in concentration between the water-filled and air-filled layers) was rapidly oxidized into CO_2 by methanotrophs under oxic conditions. In the case of CO_2, the excess CO_2 was added to the CO_2 emission streams. The addition was clearly a minor component and therefore had no significant effect on CO_2 emission. If WL were to fall from exactly the peat surface, the new air-filled layer would have a zero concentration for technical reasons. This new implementation of HIMMELI with the parameter values presented below will be referred to as HIMMELI v200 in the following text when compared to HIMMELI v1.0.1.

2.2. Site description

The measured data we used to test the model come from a nutrient-rich forested peatland, Lettosuo, located in southern Finland (60° 38′ N, 23° 57′ E; Korkiakoski et al., 2023). Prior to stem wood harvesting, the site was a Scots pine (*Pinus sylvestris*) dominated peatland, which was drained for forestry purposes in 1969. Ditches were dug with an average spacing of 45 m and a depth of about 1 m, but have since been partially filled in with growing vegetation. The undergrowth consists mainly of Norway spruce (*Picea abies*) and some silver birches (*Betula pubescens*). The forest stand was dense, with stem volumes of approximately 174, 46, and 28 m^3 ha^{-1} for Scots pine, silver birch and Norway spruce, respectively. The uneven shading of the upper canopy results in a rather patchy and variable ground vegetation, including the herbaceous species *Trientalis europaea* and *Dryopteris carthusiana*, dwarf shrubs such as *Vaccinium myrtillus* as well as the moss layer (Koskinen et al., 2014). Present peat thickness in Lettosuo varies from 1.5 m to 2.5 m (Korkiakoski et al., 2019).

SH and CC were conducted in 2016 between February 29th and March 16th in different areas in Lettosuo (Fig. 3). Details of the harvesting have been reported in previous studies (Korkiakoski et al., 2020; Korkiakoski et al., 2019). Briefly, at the SH site, 70 % of the total stem volume, including all pine trees, was harvested in an area of 13 ha. The CC was carried out on an area of 2.35 ha, where the logging residues were left on the site. The CC changed the environmental conditions of the site, and the harvesting machinery caused the destruction of the ground vegetation during the cutting. In the summer of 2017, the original ground vegetation has already been partially replaced by sun-adapted and nutrient-demanding species, such as *Rubus idaeus* and *Dryopteris carthusiana*. There is one NH site of 3.1 ha where the tree cover and ground vegetation have been left in their original state.

The long-term mean annual temperature was 4.6 °C and the mean annual precipitation was 627 mm between 1981 and 2010, measured at a nearby meteorological station ca. 35 km north-west of Lettosuo (Jokioinen Ilmala, ID: 101104; Pirinen et al., 2012). During the pre-harvest period from the year 2010 to 2015, the mean annual air temperature was 5.2 °C, ranging from 3.7 °C to 6.2 °C. The annual cumulative precipitation ranged from 568 mm to 693 mm, with an average of 636 mm. During the post-harvest period from 2016 to 2018, the annual average air temperature was 5.2 °C, 5.1 °C and 5.8 °C, and the annual accumulative precipitation was 590 mm, 773 mm and 441 m, with 2018 being extremely warm and dry (Fig. 4).

2.3. Field measurements

Two eddy covariance (EC) systems were used to measure the ecosystem-scale NEE (Korkiakoski et al., 2023). The EC measurement-based GPP was calculated for model validation. The taller EC mast (25.5 m) was used to provide data during the pre-harvest period (2010–2015) and for the SH site after the harvesting (March 2016–December 2018), while the lower EC mast (2.75 m) was used to monitor the CC site after the harvesting (April 2016–March 2018). There was no EC measurement at the NH site after harvest. The EC setup at the lower EC mast and data processing for the CC site are described in detail

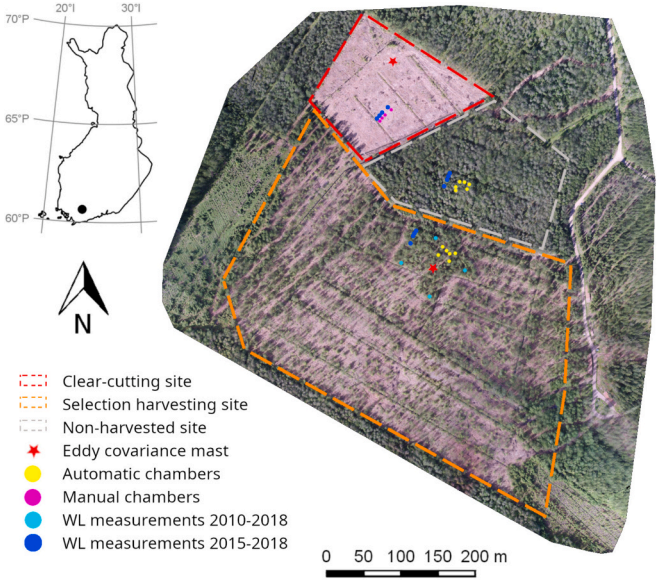

Fig. 3. Aerial view of the clear-cut site, partial-harvest site and control site at Lettosuo. The red stars show the location of the eddy covariance masts on clear-cut and partial-harvest sites, respectively. The yellow dots show the location of the automatic chambers measuring forest floor CO_2 and CH_4 fluxes from control and partial-harvest sites. The pink dots show manual chambers on the clear-cut site. The turquoise dots indicate the water level (WL) measurements operational between year 2010 and 2018, while the blue dots show WL measurements operational between year 2015 and 2018.

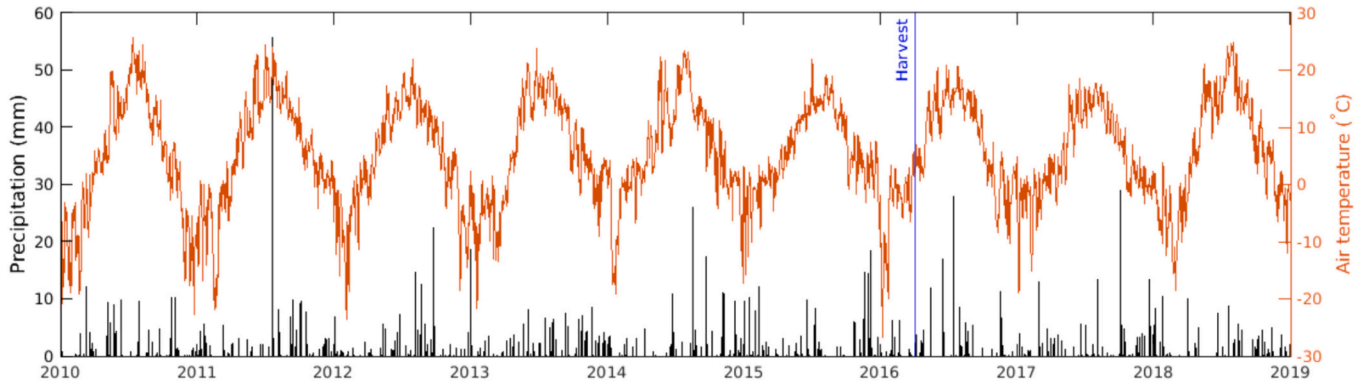

Fig. 4. Measured daily average precipitation (black) and air temperature (orange) in Lettosuo site during the pre-harvest (from January 2010 to February 2016) and the post-harvest period (from March 2016 to December 2018). The blue line indicates the time of the harvest.

in Korkiakoski et al. (2019), and for the tall mast in Korkiakoski et al. (2023). Briefly, the system at both EC masts consisted of a 3-D sonic anemometer (uSonic-3 Scientific, METEK GmbH) to measure wind components and a closed-path CO_2/H2O analyzer (Li-7000, LiCor, Inc.). Standard EC methods were used to calculate the half-hourly turbulent CO_2 fluxes for both EC systems (Aubinet et al., 2012). A detailed description of the EC data processing can be found in Korkiakoski et al. (2019, 2023) for the CC site and SH site, respectively.

Automatic chamber systems were used to measure the forest floor CO_2 and CH_4 fluxes during the pre-harvest and post-harvest periods at the NH and SH sites (Korkiakoski et al., 2020; Koskinen et al., 2014). Six transparent soil chambers were used to represent the different vegetation compositions on the forest floor. Transparent chambers measured net CO_2 flux, meaning they measured respiration only at night when no photosynthesis occurred. Therefore, to acquire respiration for the daytime and increase the temperature range for respiration modelling, the chambers were covered with blackout curtains for two to three days every two weeks during the June–August period in 2016 and 2017. These data were used to model forest floor respiration (R_{floor}) for these periods when the covers were not used, and net CO_2 flux was measured. R_{floor} was assumed to follow the Arrhenius-type model (Lloyd and Taylor, 1994):

$$R_{floor} = R_0 \times e^{\left[E\left(\frac{1}{56.02} - \frac{1}{T_{soil}-227.13}\right)\right]} \quad (4)$$

where R_0 was the forest floor respiration at 10 °C, E was the temperature sensitivity of respiration, and T_{soil} was the 5 cm soil temperature measured adjacent to the chambers (K). E and R_0 were determined separately for each period when the chambers were covered. The parameters were used to model respiration for approximately one week before and one week after the measurements from which the specific parameters were defined.

At the CC site, forest floor CO_2 and CH_4 fluxes were measured manually during the snow-free periods in 2016 and 2017 using a closed-chamber system with an opaque chamber including a mixing fan (Korkiakoski et al., 2019). The measurements were conducted once a week during the June–August period and approximately once a month during other time of the year. The CO_2 flux measured at the CC site was respiration only.

WL was measured hourly using automated probes (TruTrack WT-HR, Intech Instruments Ltd.) at four locations from May 2010 (turquoise dots in Fig. 3). Additionally, four more probes (Odyssey Capacitance Water Level Logger, Dataflow System Limited, Christchurch, New Zealand) were installed at both NH and SH sites in December 2015 and at the CC site in July 2015 (blue dots in Fig. 3). All probes measured WL on an hourly basis.

2.4. Model forcing data

We have run JSBACH offline using meteorological forcings measured at the current site, Lettosuo. The meteorological forcings used to run the JSBACH model include air temperature, air pressure, precipitation, relative humidity, wind speed, shortwave radiation and incoming longwave radiation. Briefly, air temperature (HMP45D, Vaisala Corporation), atmospheric pressure (PMT16A, Vaisala Corporation), precipitation (Casella Ltd. Par NO 10000E-04), relative humidity (HMP45D, Vaisala Corporation), wind speed (METEK USA-a, METEK GMbH) and incoming shortwave radiation (Pyranometer CMP3, Kipp & Zonen, Delft, The Netherlands) were measured on-site and were recorded as 30-min averages (Laurila et al., 2021). The missing precipitation data were filled by the measurements from the nearby weather stations operated by the Finnish Meteorological Institute: Jokioinen Ilmala (60°48′N, 23°30′E; ID: 101104) ~35 km northwest of the site and Salo Kiikala (60°27′N, 23°39′E; ID: 100967) ~ 26 km southwest of the site. These weather stations were further away from the site, which increased the uncertainties in the measurement, but it would not have had significant impacts on the model outputs as the missing values were mostly from wintertime. The missing air temperature data (8 % of the data was missing) and other meteorological data gaps were filled with measurements from Somero Salkola meteorological station (~7 km southwest of the site). Incoming longwave radiation was measured at the Tervalamminsuo mire, located approximately 1 km northeast of the study site. The model was driven with half-hourly input data while the output data were daily values.

2.5. Model parameterization

2.5.1. JSBACH model

The initial state of the JSBACH model was generated by a model spin-up, which was achieved by looping over two years of site meteorological data for 2500 years. Finally, the model status at the end of the spin-up was used as the initial status in our simulations. At the end of the spin-up, the peat depth was 1.96 m, representing the average peat depth at the experimental site (Korkiakoski et al., 2019). Initial soil carbon stocks were 92.5 kg C m^{-2}, well situated within the expected range of peatland organic matter of 50–150 kg C m^{-2} (Moore and Basiliko, 2006).

To simulate the effects of alternative harvesting regimes on ecosystem water and carbon balances, we ran the JSBACH model with different LAI_{max} for NH, SH and CC sites separately. The measured net ecosystem exchange (NEE) and gross primary production (GPP) measurement from the pre-harvest (2010–2015) and post-harvest (2016–2018) periods at each site were used to constrain the LAI_{max} values (data not shown). After optimization, we set LAI_{max} to be a constant value of 3.5 for NH throughout the post-harvest period. For SH

and CC sites, due to the rapid recovery of the understory in the first year after the harvesting (Korkiakoski et al., 2019; Leppä et al., 2020), we set LAI_{max} to be 2.5, 3, 3 at SH site and 1, 1.5, 1.5 at CC site for 2016, 2017 and 2018, respectively. The LAI used in each simulation was shown in Fig. S3.

2.5.2. HIMMELI model

We used HIMMELI v200 to simulate the soil CO_2 and CH_4 fluxes, which were the total output fluxes from diffusion and ebullition specified in the simulation. Plant transport was not considered as aerenchymatous plants, such as *Carex* spp., were rarely found growing on the floor of peatland forest floor. HIMMELI received the outputs from JSBACH as its own inputs, including peat temperature, air temperature, WL, and soil anaerobic respiration rate (Fig. 5). Prior to each simulation, HIMMELI v200 was looped 50 times over three years (2016–2018) to obtain stabilized soil gas concentrations.

The soil CO_2 flux from the HIMMELI output represented the heterotrophic soil respiration. Note that JSBACH also simulated both oxic and anoxic soil respiration; however, we used the HIMMELI output as the final soil CO_2 flux in this work because HIMMELI included the CO_2 flux produced by CH_4 oxidation, which was not included in JSBACH.

The model parameters for CH_4 production and oxidation were modified and the remaining model parameter values were adopted from Raivonen et al. (2017). *fm* indicated the percentage of CH_4 production rate compared to anaerobic respiration rate in the absence of dissolved O_2 at a given depth. The *fm* was set at 0.06, which is at the lower end of the theoretical range of the fraction of CH_4 yield from soil organic matter under optimal methanogenic conditions (0 to 0.7; Nilsson and Öquist, 2009), as the lower water level in the peatland forest sites could have greatly limited CH_4 production. This value of *fm* was supported by a parameter optimization work, where model parameters were constrained by data on soil CH_4 and CO_2 concentration profiles and surface fluxes in Lettosuo during the post-harvest period (Leppänen et al., unpublished). The aerobic soil respiration at a reference soil temperature of 10 °C was set to be 3×10^{-6} mol m^{-3} s^{-1}, the mean value of the reference heterotrophic respiration rate in different peatland forests in Finland (Ojanen et al., 2010). Measured CH_4 oxidation potentials from the upper 30 cm of soil at Lettosuo ranged from 1.3×10^{-6} to 1.5×10^{-5} mol m^{-3} s^{-1} for low-affinity methanotrophs at the SH site (unpublished data from A. Putkinen). In our study, we used oxidation potentials from the upper end of the measurement range, as generally low water level in peatland forests should favour higher CH_4 oxidation (Ojanen et al., 2010). The Michaelis constant for CH_4 in oxidation was set at 0.015 mol m^{-3} following Stephen et al. (1998).

The soil layer divisions in HIMMELI were set to the same level as used in JSBACH, where the lower limit of each layer from top to bottom was 0.06, 0.19, 0.45, 0.97 and 2 m (the layer thicknesses were 0.06, 0.13, 0.26, 0.52, 1.03 m from the surface).

2.6. Model performance

We used the following specific data streams in JSBACH to evaluate the model performance: WL, NEE and GPP. WL (m) is the height of free water in the soil (positive value means above the soil). NEE and GPP (μmol CO_2 m^{-2} s^{-1}) represent the net carbon exchange and photosynthesis at the ecosystem level. We compared these simulated variables with the daily average of observations from both the pre-harvest and post-harvest periods. Only days where the number of accepted half-hourly data after data screening was greater than or equal to 24, i.e., the daily data coverage was ≥50 %, were included in the analysis. We then compared the simulated soil CO_2 and CH_4 fluxes from HIMMELI with the observations from chamber measurements during the post-harvest period, i.e., from March 2016 to December 2018 (Korkiakoski et al., 2017, 2019, 2020). We used RMSE (Root Mean Square Error) and *Pearson's r* (Pearson correlation coefficient) to quantify the differences and the correlations between the model prediction and the observations.

As the soil CO_2 flux measured by dark chambers was only available from June to August in 2016 and 2017, the model-measurement comparisons for CO_2 flux were only performed during these periods. Furthermore, the CO_2 flux from HIMMELI represented the heterotrophic respiration (R_{het}), while the chamber-measured CO_2 flux represented the forest floor respiration (R_{floor}), which included autotrophic respiration (R_a) from ground vegetation and living roots, R_{het} from soil organisms and decomposition of dead roots (R_d). For a justified comparison, the modelled CO_2 fluxes from HIMMELI were divided by a monthly average percentage contribution of R_{het} to R_{floor} for both NH and SH sites, following Pumpanen et al. (2015). The percentage of contribution of R_{het} was highest in winter (December to March, 95 %) and lowest in summer (55 %), corresponding to the increasing contribution of R_a from winter to summer. Although R_a was very small at the CC site, R_d was reported to account for 43–53 % of R_{floor} (Ngao et al., 2007). We took an average of 48 % as the contribution of R_d to R_{floor} and the remainder (52 %) as the contribution of R_{het} to R_{floor}. The seasonal and interannual variation of R_d was not considered in our calculations.

To illustrate how the peatland forest soil behaves as a source or a sink of GHG equivalents after different harvesting operations, we also calculated the sustained global warming potential of CO_2 and CH_4 over a 100-year horizon at each site ($SGWP_{-100}$; Neubauer and Megonigal, 2015). Unlike the conventionally used global warming potential, which treats emissions as a one-time pulse, $SGWP_{-100}$ assumes persistent emissions to account for the effect of GHG remaining in the atmosphere during this period. In practice, we have multiplied the CH_4 flux by a factor of 45 to convert it to g CO_2-eq m^{-2} yr^{-1}.

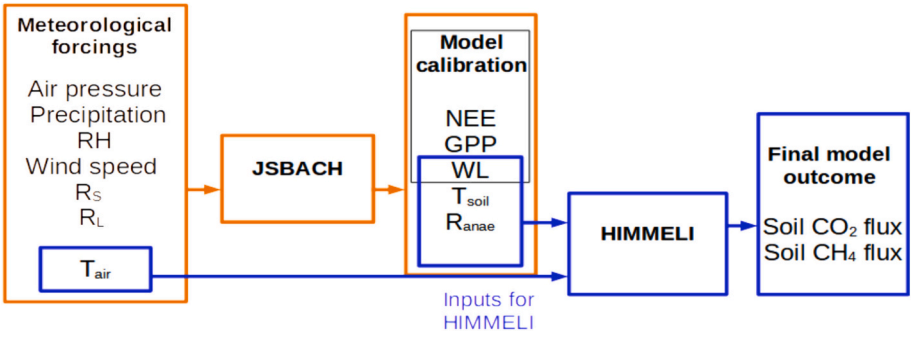

Fig. 5. Schematic figure of JSBACH-HIMMELI model framework in simulating forest floor CO_2 and CH_4 fluxes from peatland forest. RH — relative humidity; R_S — shortwave radiation; R_L — longwave radiation; T_{air} — air temperature; WL — water level; T_{soil} — soil temperature; R_{anae} — soil anaerobic respiration. Note that for simplicity, the leaf area index of aerenchymatous plants (another input for HIMMELI), was assumed to be zero, as the main species in the ground vegetation of Lettosuo were not aerenchymatous (Korkiakoski et al., 2023).

3. Results

3.1. Pre-harvest period

During the pre-harvest period (years 2010–2015), simulated monthly and daily NEE and GPP agreed well with the daily average of measured NEE and GPP (Figs. 6 and S4). For NEE, $r = 0.71$, RMSE = -1.73 μmol CO_2 m^{-2} s^{-1} and for GPP, $r = 0.89$ and RMSE = 1.99 μmol CO_2 m^{-2} s^{-1}.

The simulated daily WL generally captured the seasonal dynamics of the measured WL ($r = 0.82$, RMSE = 0.08 m), while some high and low extremes in the measurements were not represented in the model (Fig. 7). The largest discrepancies between the model and the measurements occurred in the periods when the measured WL showed high extremes in the winter and spring. There was a large inter-annual variability of WL, reflecting the effects of meteorological parameters during the pre-harvest period. The measured annual averages of WL (±standard deviation) were −0.46 (±0.14) m, −0.42 (±0.13) m, −0.37 (±0.13) m, −0.43 (±0.14) m, −0.37 ± (0.09) m and −0.38 (±0.15) m between year 2010 and 2015, with the highest values in the spring up to −0.10 m and the lowest values in the summer down to −0.70 m. The modelled annual averages of WL (±standard deviation) were −0.45 (±0.08) m, −0.45 (±0.06) m, −0.42 (±0.08) m, −0.45 (±0.08) m, −0.40 (±0.06) m, −0.39 (±0.07) m between year 2010 and 2015.

3.2. Post-harvest period

3.2.1. Ecosystem CO_2 fluxes and variation of soil water level

After the forest harvest, both measured and modelled ecosystem CO_2 fluxes responded to the alternative harvesting regimes applied at each site (Fig. 8). The NEE from the SH site showed smaller negative values compared to the simulation from the control site, while at the CC site the NEE appeared to be positive during the peak growing seasons. The modelled monthly averages of NEE were systematically smaller than the measured ones for the CC site (Fig. 8a). The correlations between modelled and measured NEEs were weaker at both the SH site (Fig. S5a; $r = 0.42$, RMSE = 1.43 μmol CO_2 m^{-2} s^{-1}) and the CC site (Fig. S5b; $r = 0.71$, RMSE = 1.32 μmol CO_2 m^{-2} s^{-1}). The modelled GPPs correlated well with the measurement-based GPPs at both the SH site (Fig. S5c; $r = 0.88$, RMSE = 1.42 μmol CO_2 m^{-2} s^{-1}) and the CC site (Fig. S5d; $r = 0.84$, RMSE = 0.48 μmol CO_2 m^{-2} s^{-1}). GPPs became more negative, indicating greater CO_2 uptake, from 2016 to 2018 in both the SH and CC sites (Fig. 8b).

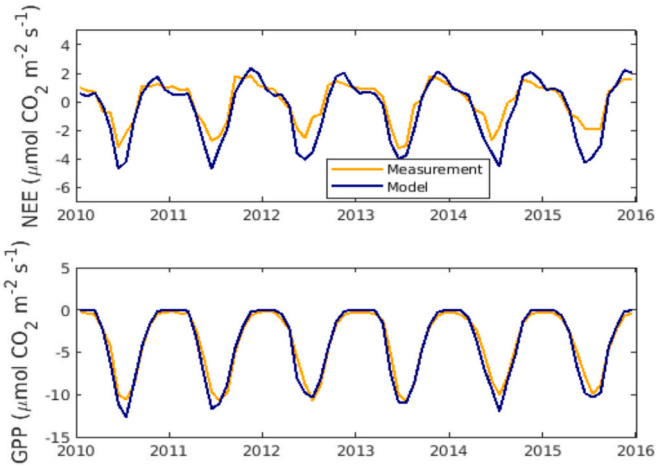

Fig. 6. Seasonal dynamics of (a) net ecosystem exchange, NEE and (b) gross primary productivity, GPP, during the pre-harvest period (year 2010–2015). Yellow and blue lines show monthly-averaged measurement and model simulation.

Large variability was observed in the measured daily WL, which ranged between −88.1 cm and −16.6 cm, −81.6 cm and −7.9 cm, −51.8 cm and −3.0 cm at NH, SH, and CC sites, respectively. The simulated WL captured well the seasonal and interannual variations in the observed WL and the associated harvesting effects. The correlation coefficient r between the measured and modelled WL was 0.85, 0.88 and 0.72, and the RMSE was 8.1, 8.4 and 5.5 cm at the NH, SH, and CC sites, respectively (Table 1; Fig. 9). After harvest, the measured WL from May to September was on average 18 cm higher at the CC site and 5 cm higher at the SH site compared to the NH site (Leppä et al., 2020). Similarly, the modelled WL during the same period was elevated by 19.6 cm at the CC site and 6.5 cm at the SH site. During the dry year 2018, the WL was significantly affected at NH and SH sites, decreasing to −77.6 cm and −69.4 cm, respectively. The model was able to capture the extremely low WL during the summer of 2018, where the modelled WL reached −75.2 cm and −71.3 cm at the NH and SH sites, which were ~30 cm lower than the modelled WL at the CC site.

3.2.2. Soil CH_4 and CO_2 fluxes

The updated model captured the observed patterns of soil CH_4 from the peatland forest after the harvest operations. At both NH and SH sites, the model showed CH_4 uptake during the summer as observed in the measurements. The correlation coefficient r of the model-data comparison was on average 0.73 for the NH site and 0.76 for the SH site (Fig. 10a and c; Table 1). On average, the modelled annual mean CH_4 flux at the NH site was −0.44 and −0.34 nmol m^{-2} s^{-1} for the years 2016 and 2017, which were close to the measured annual mean CH_4 fluxes of −0.40 and −0.34 nmol m^{-2} s^{-1} in the respective years. At the SH site, CH_4 uptake was highest in 2018 due to the extremely dry summer. The annual mean CH_4 fluxes were −0.46, −0.39, −0.49 nmol m^{-2} s^{-1} in the model and −0.25, −0.18, −0.42 nmol m^{-2} s^{-1} from the measurement for the years 2016, 2017 and 2018, respectively. There were occasional CH_4 emission peaks in the measured data, e.g., in winter 2017 at the NH site and in summer 2018 at the SH site, which were not simulated by the model. At the CC site, we compared modelled and measured CH_4 fluxes from June to August in 2016 and 2017 due to the availability of data from the manual measurements. Both the model and the measurements showed that the site was generally a small source of CH_4 during this period. The average modelled CH_4 fluxes were 0.45 and 0.53 nmol m^{-2} s^{-1} between June and August in 2016 and 2017 and they were 0.42 and 0.52 nmol m^{-2} s^{-1} from the measurements (Table S2). There were differences in the emission patterns: measurements showed that the soil was a small CH_4 source constantly throughout the summer, while both CH_4 uptake and emission were simulated by the model, and the emission peaks occurred mainly in summer in the form of diffusion caused by ebullition (Fig. 10e).

For soil CO_2 fluxes (i.e., R_{het}), we compared the model simulation with the measurements between June and August in 2016 and 2017 (due to data availability). The mean correlation coefficients r was 0.75 and 0.69, and the RMSE was 0.865 and 0.882 μmol m^{-2} s^{-1} for the NH and SH sites, respectively (Fig. 10b and d). At the CC site, the mean soil CO_2 fluxes from the measurements were slightly higher than the mean simulated CO_2 fluxes, but there were no significant differences (Fig. 10f; Table 2). As simulated by the model, the annual accumulated R_{het} was on average 1361, 1311 and 930 g CO_2 m^{-2} yr^{-1} from the NH, SH and CC sites in 2016 and 2017, respectively (Table 3). The simulated R_{het}, was from the NH peatland forest site was 1372 and 1350 g CO_2 m^{-2} yr^{-1} in year 2016 and 2017, respectively. These values were well within the range of R_{het} (535–2455 g CO_2 m^{-2} yr^{-1}) reported in a previous study that included 68 forest drained peatland sites in Finland (Ojanen et al., 2010).

The model simulated a trade-off between soil CH_4 and CO_2 fluxes regulated by WL under different harvesting regimes. It showed that increasing WL, which was beneficial for CH_4 production and inhibits CH_4 uptake, would reduce soil CH_4 uptake (or increase soil CH_4 emissions) and reduce soil CO_2 emissions. Compared to the baseline model

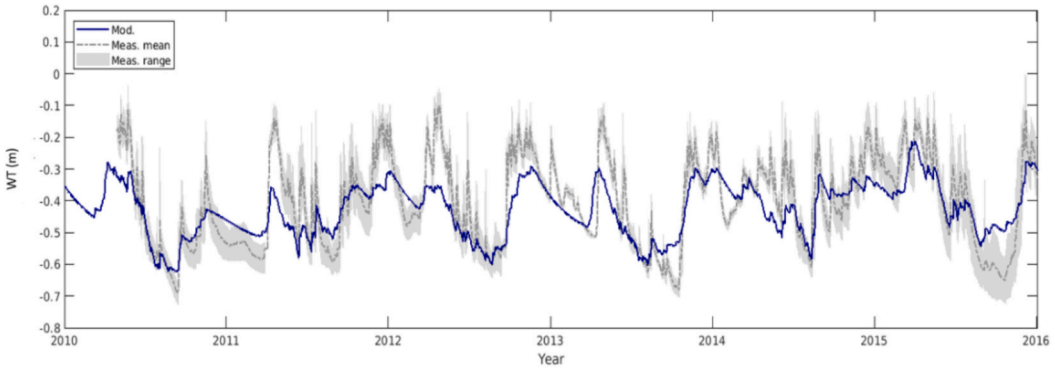

Fig. 7. Measured and modelled seasonal dynamics of daily WTD during pre-harvest period (2010–2015). Blue line shows simulated daily WTD. Grey area indicates the maximum and minimum of the daily averages of the measurements from the four loggers. Grey line shows the mean of the daily averages of the measurement.

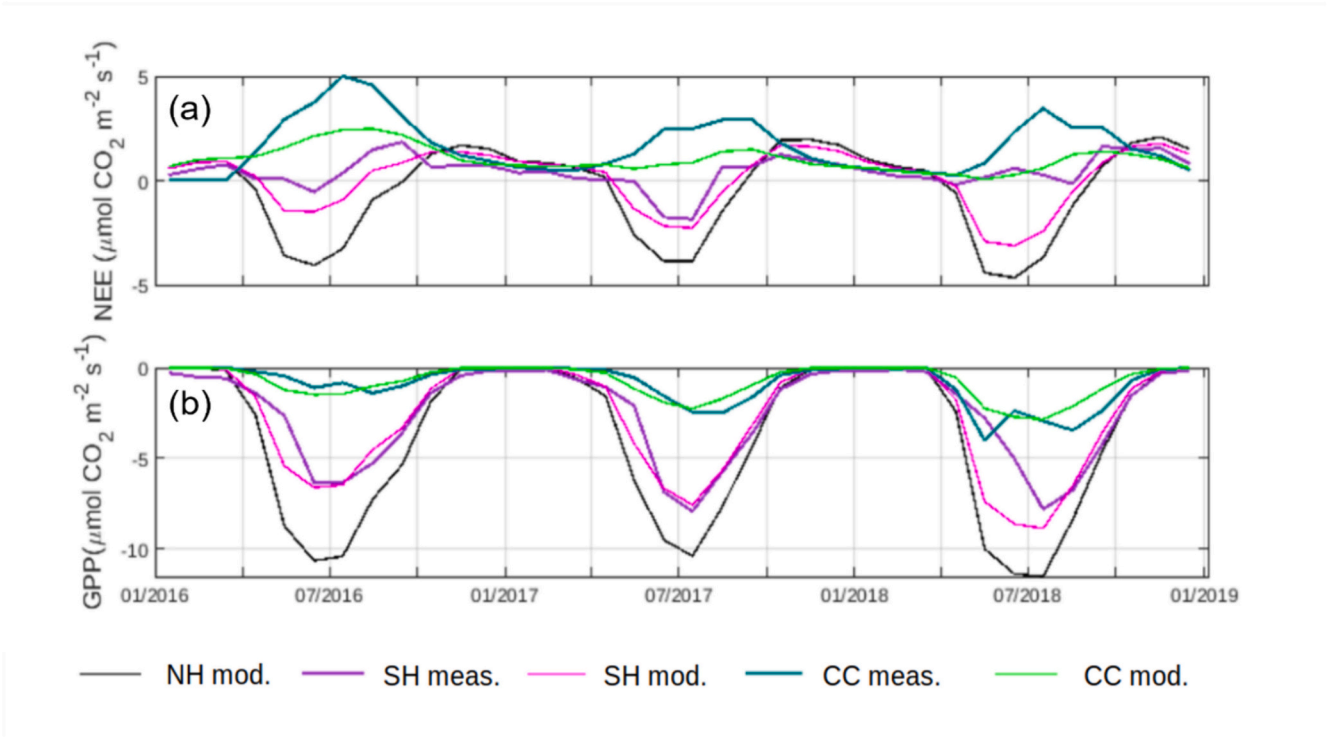

Fig. 8. The monthly mean of measured (meas.) and modelled (mod.) net ecosystem exchange, NEE (a) and gross primary productivity, GPP (b) at selection harvesting (SH) and clear-cutting (CC) sites during the post-harvest period (year 2016–2018). Model prediction of fluxes from the non-harvested (NH) site are presented as reference (black lines).

where the water table of the NH site was applied (−45 cm on average), when the WL was increased by 40 cm with 10 cm increments, the annual soil CH_4 uptake decreased by 23.2 %, 44.7 %, 73.8 %, 93.9 %, while the annual soil CO_2 emission decreased by 21.4 %, 44.2 %, 65.1 % and 84.3 % (Fig. S6).

Soil CH_4 emissions increased and soil CO_2 emissions decreased as the amount of tree cover on the site decreased, i.e., from the NH site, to the SH site and to the CC site. However, the magnitude of the decrease in CO_2 flux was much greater than that of the increase in CH_4 flux when comparing the CO_2 equivalents of these two gases (Table 3). The decrease of the simulated annual CO_2 fluxes between the NH and the CC site was 413 and 449 g CO_2 m^{-2} yr^{-1}, while the increase of the CH_4 flux was 0.182 and 0.225 g CH_4 m^{-2} yr^{-1}, corresponding to 8.18 and 10.1 g $CO_{2\text{-eq}}$ m^{-2} yr^{-1} in the year 2016 and 2017, respectively.

4. Discussion

In this paper we modified and applied JSBACH-HIMMELI models to simulate the effects of alternative harvesting on water level (WL), ecosystem fluxes, and soil CH_4 and CO_2 fluxes from a peatland forest. Several years of measured data were used to calibrate the models and evaluate their performance. Our model demonstrated a GHG trade-off between soil CH_4 and CO_2 fluxes under alternative forest harvesting. According to our results, the radiative forcing of peatland forest soil decomposition is determined by CO_2, despite its low GWP.

In the original $YASSO_{peatland}$, WL was controlled by the equilibrium evapotranspiration but we set WL to follow soil moisture that is influenced by the evapotranspiration intensity of the forest stand (Leppä et al., 2020). Furthermore, we introduced new parameters in the formula to enable simulating the overall level and range of variation of WL, dependent on LAI_{max}. Both the original HIMMELI v1.0.1 and the new HIMMELI v200 correctly simulated the annual average of CH_4 uptake at

Table 1
The Pearson correlation coefficient (*r*) and the Root Mean Square Error (*RMSE*) between the modelled and measured water level (WL), CH_4 flux and CO_2 flux at the non-harvested, selection harvesting and clear-cutting sites during the post-harvesting years. CH_4 and CO_2 fluxes were measured with automatic chamber at the non-harvested and selection harvesting sites. There were only a few manual measurements taken at the clear-cutting site, thus the *r* and *RMSE* were not presented.

	WL		CH_4		CO_2	
	r	*RMSE* (cm)	*r*	*RMSE* (nmol m^{-2} s^{-1})	*r*	*RMSE* (μmol m^{-2} s^{-1})
Non-harvested						
2016	0.81	7.3	0.84	0.19	0. 71	0.41
2017	0.77	9.4	0.61	0.28	0. 79	1.32
2018	0.94	7.4	–	–	–	–
All years	0.84	8.1	0.73	0.24	0.75	0.87
Selection harvesting						
2016	0.63	7.4	0.91	0.20	0.67	0.34
2017	0.77	10.2	0.57	0.22	0.72	1.42
2018	0.97	7.2	0.79	0.24	–	–
All years	0.79	8.4	0.76	0.22	0.70	0.88
Clear-cutting						
2016	0.36	6.1	–	–	–	–
2017	0.71	5.4	–	–	–	–
2018	0.82	5.1	–	–	–	–
All years	0.63	5.5	–	–	–	–

the NH and SH sites, and CH_4 emission at the CC site during the post-harvest years (Table S2), showing that the model results were consistent and robust. However, although HIMMELI v1.0.1 could reproduce the CH_4 fluxes from the peatland forest in terms of annual balance, HIMMELI v200 was a more suitable tool for simulating the observed CH_4 time series, especially when CH_4 uptake was present.

Peatland CH_4 and CO_2 fluxes and also their trade-off due to changes in WL as a response to management have been modelled previously (Shanin et al., 2021; Huang et al., 2021). However, to our knowledge, this is the first time to adapt a process-based model, that simulates the vertical distribution of biogeochemistry and concentrations of CH_4, O_2 and CO_2, for that purpose. In general, modelling studies focusing on the GHG fluxes of drained peatlands where the CH_4 flux is close to zero and can alternate from positive to negative, depending on conditions, are scarce.

4.1. Model modifications in HIMMELI for peatland forest

In HIMMELI v1.0.1, dissolved gas was left in the new air-filled peat layer as WL decreased, creating artificial CH_4 peaks. Similarly, Tang et al. (2010) and Walter and Heimann (2000) reported that their models predicted increasing CH_4 diffusion from the soil induced by decreasing WL and increased concentration gradient. In contrast, HIMMELI v200 assumed that the excess CH_4 was immediately oxidized to CO_2 (Fig. 2). The amount of oxidized excess CH_4 was small, accounting for only 12 %, 13 % and 3 % of the CH_4 production at the NH, SH and CC sites, respectively (Fig. S7). The resulting increase in CO_2 flux after CH_4 oxidation was also small.

In reality, water moves not only vertically but also horizontally,

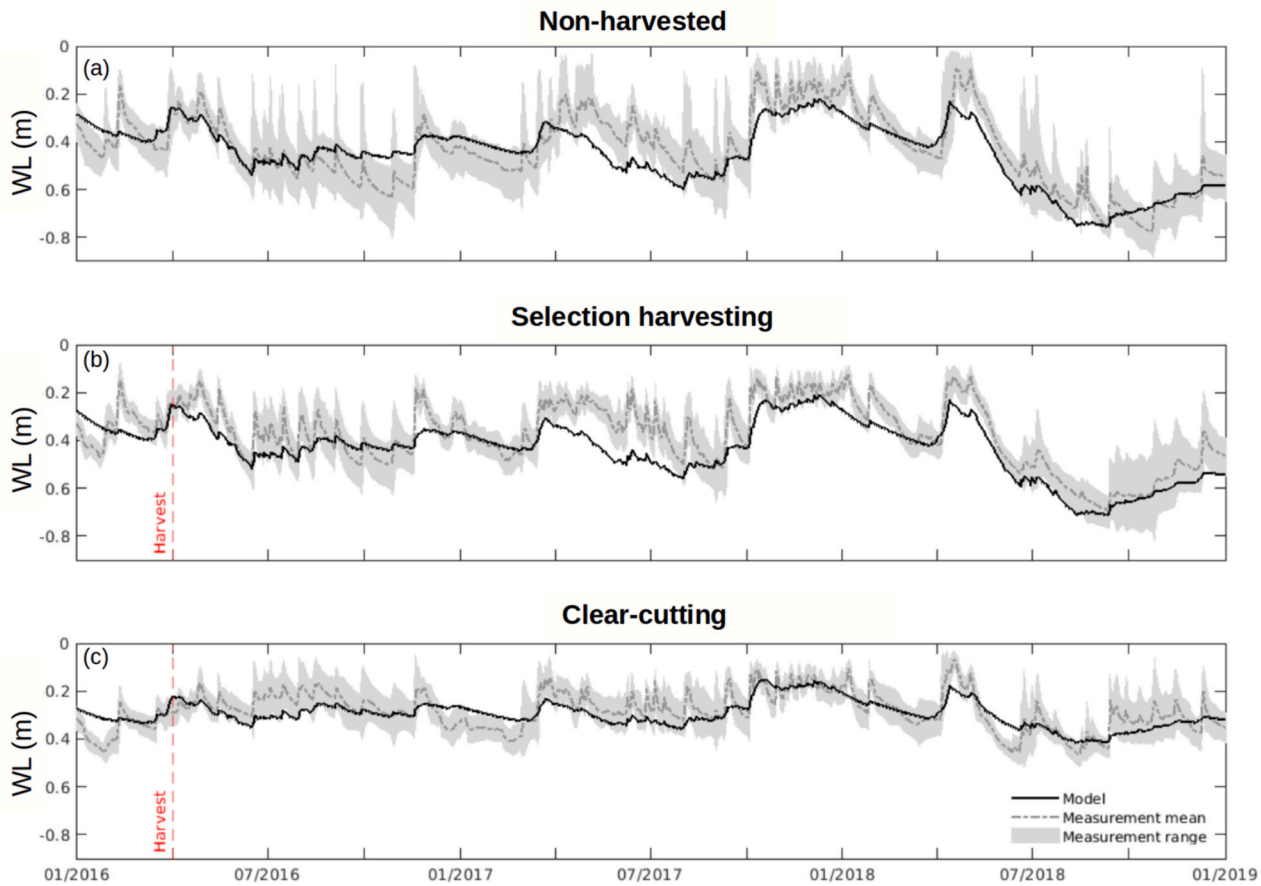

Fig. 9. Comparison of simulated and measured post-harvest water level (WL) at (a) non-harvested, (b) selection harvesting and (c) clear-cutting sites. Solid lines represent the modelled daily averaged WL. Dash-dotted lines and shaded areas represent the daily means of the measurement and the measurement range due to spatial variations. The red dashed lines indicate the time of the forest harvesting at selection harvesting and clear-cutting sites.

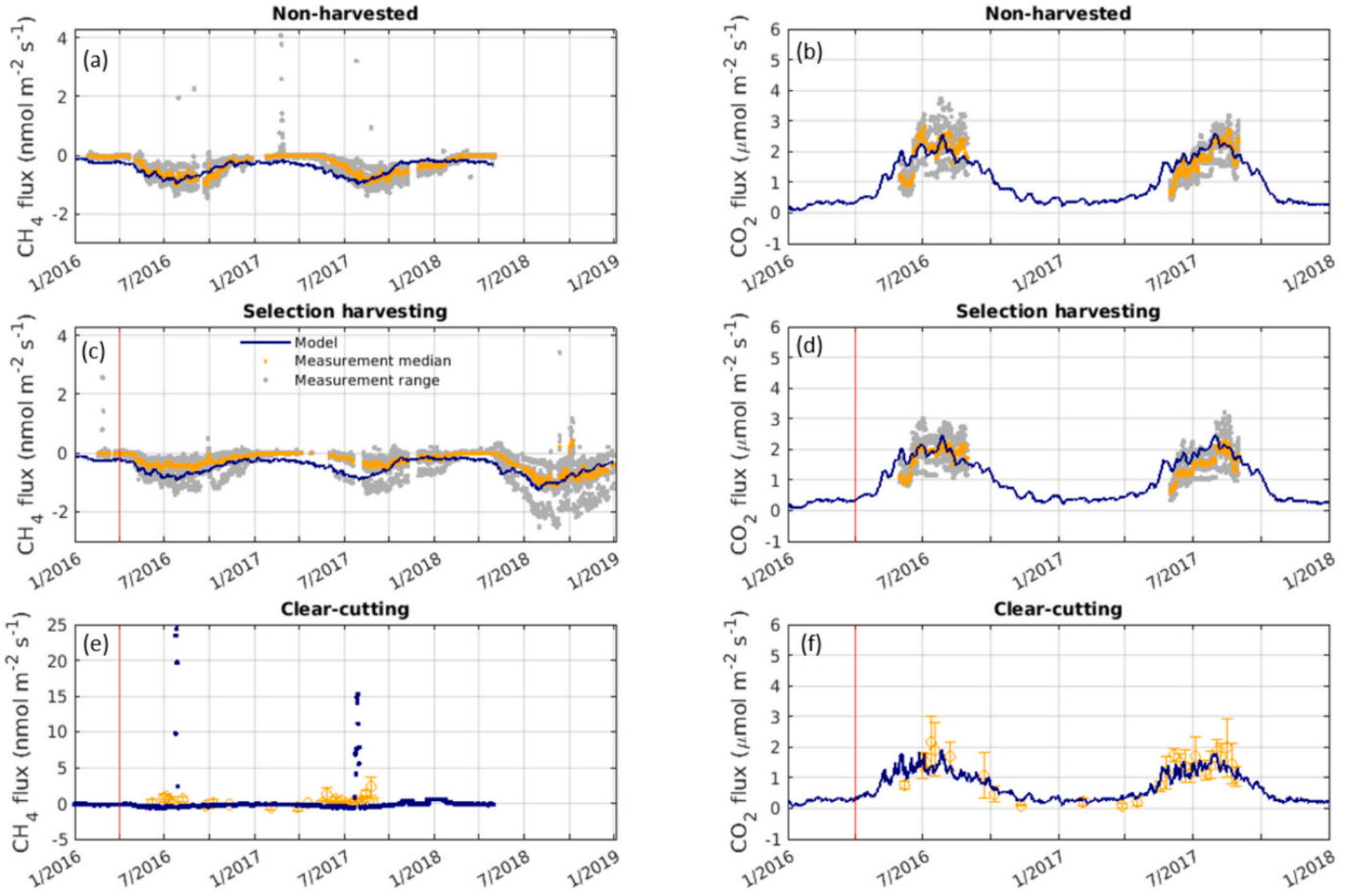

Fig. 10. Measured and modelled CH_4 (left panels) and CO_2 (right panels) fluxes from the forest floor in non-harvested (a and b), selection harvesting (c and d) and clear-cutting sites (e and f) during the post-harvest period. Blue dots show daily CH_4 and CO_2 fluxes simulated by HIMMELI-veer. For a, b, c and d, grey dots represent the daily average of fluxes measured by each of the six automated chambers and yellow lines show a median value of these daily measurements. For e and f, yellow circles and error bars represent the daily means and standard deviations of CH_4 and CO_2 fluxes measured by manual chambers. Red lines indicate the time of forest harvest.

Table 2
The mean and standard deviation of measured and modelled CO_2 fluxes during the peak growing seasons in 2016 and 2017 after the harvesting (unit: μmol CO_2 m^{-2} s^{-1}).

		Non-harvested	Selection harvesting	Clear-cutting
2016	Measurement	1.98 ± 0.52	1.79 ± 0.38	1.57 ± 0.49
	Model	1.95 ± 0.28	1.87 ± 0.28	1.30 ± 0.24
2017	Measurement	1.78 ± 0.49	1.51 ± 0.37	1.51 ± 0.29
	Model	1.99 ± 0.31	1.90 ± 0.30	1.30 ± 0.22

especially in a peatland forest with an extensive ditch system exists. Sarkkola et al. (2013) found that in a peatland forest in Finland, 6 — 44 % of the total annual precipitation was discharged as runoff. The drainage ditches are local hotspots for CH_4 emissions, as they are usually wet areas, and the majority of CH_4 fluxes from the ditch have been observed to be transported by drainage water from the surrounding areas. In addition, dissolved soil gas such as CH_4 can also be transported to the standing vegetation and be released by transpiration. These above-mentioned processes, especially lateral gas transport, are not yet included in the current version of HIMMELI, a one-dimensional, vertically layered peat column CH_4 model, nor in other CH_4 modelling schemes. The detailed simulation of these processes and the separation of the roles of transpiration, evaporation, runoff, etc. in CH_4 transport with detailed hydrological characteristics and environmental conditions of the drainage system are beyond the scope of the current study.

Although our modification of the models captured the major changes in soil CH_4 and CO_2 fluxes induced by forest harvesting, the model predictability could be improved in the following aspects. The current version of $YASSO_{peatland}$ does not include the additional litter input into the soil carbon pool after forest harvesting, which may lead to an underestimation of ecosystem respiration (R_{eco}). Previous studies have shown high R_{eco} in the peatland forest after forest harvesting due to the

Table 3
Comparison of the simulated annual accumulative soil CH_4 flux, its CO_2-equivelant and the annual accumulative soil CO_2 flux, i.e. heterotrophic soil respiration at the non-harvested (NH), selection harvesting (SH) and clear-cutting (CC) sites during the post-harvest years.

	CH_4 (g CH_4 m^{-2} yr^{-1})			CH_4 (g CO_2-eq m^{-2} yr^{-1})			CO_2 (g CO_2 m^{-2} yr^{-1})		
	2016	2017	2018	2016	2017	2018	2016	2017	2018
NH	−0.222	−0.220	–	−9.99	−9.90	–	1372	1350	–
SH	−0.221	−0.207	−0.275	−9.93	−9.31	−12.37	1328	1294	–
CC	−0.040	0.005	–	−1.81	0.20	–	959	901	–

high amount of easily decomposable organic matter, e.g., dying vegetation and tree roots, as well as logging residuals left on site (Mäkiranta et al., 2010; Yang et al., 2022). Similarly, in our study, the modelled GPP after CC was in good agreement with the measurement-based GPP, but the modelled NEE was consistently smaller than the measured ones (Fig. S5b and d), indicating an underestimation of R_{eco} by the model. Therefore, the inclusion of dynamic forest growth and clear-cut cycles that mechanistically accounts for the effects of changes in litter input on soil carbon would improve the model prediction, and a study including these features is in preparation (Tyystjärvi et al., 2024). Furthermore, the current model version predicted CH_4 uptake from the end of March, while measurements showed noticeable CH_4 uptake only from May after soil thawing in 2017 for both NH and SH sites (Fig. 10a and c). This discrepancy may be attributed to the ice and snow effects. A layer of snow and ice could largely prevent the gas exchange between the atmosphere and the soil (Melloh and Crill, 1996; Comas et al., 2008), thus delaying CH_4 uptake. The snow/ice layer could also reduce the fast diffusion of oxygen (O_2) into the soil to oxidize the CH_4 produced during winter, so the high concentration of CH_4 under the snow could reduce the sink strength of CH_4 in the soil. The ice/snow implementation of HIMMELI is currently under development (Raivonen et al., unpublished).

4.2. Modelling the harvesting impacts on environmental variables

WL is an important environmental variable as it determines the ratio of aerobic and anaerobic processes in the peatland soil and the soil decomposition rate (Päivänen and Hånell, 2012). The new parameters that we introduced into the WL model, *m* and *n,* were linked to LAI_{max} by an asymptotic exponential equation, as the effect of transpiring forest levels off with increasing stand volume (Eq. (2); Fig. S1). For example, Sarkkola et al. (2010) found that the effect of tree stand on WL was most steep when stand volume was between 10 and 100 m^3 ha^{-1} and it became minimal when stand volume exceeded 200 m^3 ha^{-1}. At the study site, the total stem volume before the harvesting was about 240 m^3 ha^{-1} (Korkiakoski et al., 2023).

Soil temperature (T_{soil}) is another important environmental variable that determines soil respiration in a peatland forest (Mäkiranta et al., 2008). T_{soil} at the surface can increase after forest harvesting as more direct solar radiation reaches the forest floor (Korkiakoski et al., 2020). As expected, both measured and modelled T_{soil} were higher at the CC site than at the NH site, but the measurements showed greater differences among the sites (Table S3). For example, the difference in mean T_{soil} (5 cm belowground) between the NH and CC sites during June–August in 2017 could reach as much as 0.5 °C, compared to the 0.15 °C in the model simulation. As T_{soil} has a positive effect on soil decomposition rate, the underestimation of the increase in T_{soil} after CC contributed to the model's underestimation of CO_2 flux at the CC site (Table 2).

4.3. Modelling the harvesting impacts on soil GHG emissions

Our model has demonstrated the effects of harvesting on soil CH_4 and CO_2 fluxes from the peatland forest through varying WL, which was affected by the amount of tree cover on the site (Fig. 10). The simulated dependence of soil CH_4 and CO_2 on WL in peatland forests was consistent with previous empirical (e.g., Ojanen and Minkkinen, 2019) and modelling (e.g., Shanin et al., 2021) studies. Previous research also found that the dependence of soil CO_2 on WL ceased when WL increased above a critical threshold, approximately −10 cm below the surface (Waddington and Roulet, 2000), or when WL reached and exceeded −70 cm below the surface (Mäkiranta et al., 2009). However, this is rarely the case in boreal peatland forest. Furthermore, Jungkunst and Fiedler (2007) found that there was a latitudinal trend in the reduction of CO_2 emission with increasing WL, where we would expect the effect to be more pronounced in the warm tropical condition, as well as in the temperate peatlands (Couwenberg et al., 2011). This shows that we need to consider the complexity of the climatic conditions and vegetation when simulating soil GHG emissions in peatland forests beyond the boreal region.

Combining the dependence of water table on tree cover and the dependence of soil CO_2 and CH_4 fluxes on water table in the peatland forests, we demonstrated the opposite effects of harvesting on soil CH_4 and CO_2 fluxes in peatland forests (Figs. 10 and S8). In Fig. S8, positive values indicated emission (gas moving from soil to air) and negative values indicated uptake (gas moving from air to soil). Different values of LAI_{max} indicated harvesting options, with 3.5, 2.5 and 1.5 corresponding to NH, SH and CC, respectively. Soil CH_4 uptake was reduced and soil CH_4 emission increased as harvest intensity increased (lower LAI_{max}) due to higher soil moisture and anoxic respiration, while the soil CO_2 emission was reduced due to lower aerobic soil decomposition. When LAI_{max} was low (intensive harvesting), the change in soil CH_4 flux or soil CO_2 flux was much more pronounced than when LAI_{max} was high (light harvesting; Fig. S8). Recent global meta-analyses have shown that the intensity of forest harvesting is important for predicting CH_4 and CO_2 emissions (Yang et al., 2022; Zhang et al., 2018). Under light harvesting, higher thinning intensity increased CO_2 emission, which could be attributed to the increased soil temperature after harvesting and the increased litter input from dead roots and thinning residues. Meanwhile, the reduced litter fall would have the opposite effect on soil CO_2 emissions. Therefore, the overall effect may be unchanged.

4.4. Model implications

Both the model simulation and the measurements showed a trade-off between soil CO_2 and CH_4 fluxes from the peatland forest under the alternative harvesting regimes: there was more soil CO_2 emission and less soil CH_4 emission at the SH site, and vice versa at the CC site (Fig. 10). Although CH_4 has a much higher global warming potential, we found that soil CO_2 is the dominant forcing in terms of radiative forcing from the peatland forest soil when comparing between alternative harvesting regimes (Table 3), as has been found previously in other studies previously (Günther et al., 2020; Jungkunst and Fiedler, 2007). This indicates that the peatland forest soil is a stronger carbon source after selection harvesting, as used in CCF, compared to clear-cutting, as used in EM. However, if we consider the change in ecosystem carbon balance under alternative harvesting regimes, including the carbon stock of the trees, the picture would change drastically. A previous study found that both harvesting regimes turned the Lettosuo forest from CO_2 neutral to a CO_2 source immediately after the harvest, but the forest after SH became a CO_2 sink a few years later, while it remained a CO_2 source after CC (Korkiakoski et al., 2023).

The general applicability of such a modelling tool to other boreal peatlands would require further testing. Our model was calibrated using data from a nutrient-rich peatland forest, which may not be equally applicable to nutrient-poor peatland forests, as they have different environmental characteristics and carbon balances (Martikainen et al., 1995). Nutrient-poor environments are in favour of the presence of bryophytes, which have lower decomposability when compared to vascular plants, leading to higher soil carbon accumulation (Kasimir et al., 2021). The dependence of soil CH_4 and CO_2 fluxes on water level changes was more pronounced in nutrient-rich sites than in nutrient-poor sites (Ojanen and Minkkinen, 2019). CH_4 production and oxidation potential in peatland forests also vary with many factors such as peat depth, substrate availability, presence of alternative electron acceptors, oxygen availability and redox potential etc. (Lai, 2009). Therefore, CH_4 flux under alternative harvesting regimes could be highly variable depending on the characteristics of the peatland forest, and further studies are needed to assess the model predictability under a wider range of ecosystem and climate conditions.

5. Conclusions

In this study, we applied simple modifications to JSBACH-HIMMELI model and tested the model against measurements of ecosystem CO_2 fluxes, WL, and soil CO_2 and CH_4 flux data from a nutrient-rich peatland forest in southern Finland during the pre-harvest years 2010–2015 and the post-harvest years 2016–2018. The results showed that our model framework was robust: by relating WL to the soil moisture and the maximum leaf area index as well as the scaling parameters, the model could reproduce the CO_2 and CH_4 fluxes from peatland forest soil under alternative harvesting regimes with reasonable accuracy compared to observations. Further research including the snow/ice effect, dynamic forest growth, litter input on soil carbon status and site-specific characteristics would improve the applicability and predictability of the model.

Regarding the three hypotheses formulated in the introduction, we conclude that:

(1) Our model reasonably represented the seasonal variation of WL affected by alternative forest harvesting, although there were discrepancies between model and measurement when extreme values occurred, e.g. during soil thawing in spring.
(2) With the same parameterization, our model was able to simulate the soil CH_4 uptake in the NH and SH site as well as the CH_4 emission in the CC site as observed in the measurement.
(3) Our model showed a dynamic trade-off between the soil CH_4 flux and the soil CO_2 flux based on the increase or decrease in WL induced by different harvesting options. At the SH site with low WL, there was lower CH_4 emission and higher CO_2 emission (soil respiration), and vice versa at the CC site. In terms of soil carbon balance, the CH_4 reduction at the SH site was outweighed by the increase in soil CO_2 flux during the first three years after the harvest. In the long term, however, the reduction of climatic impacts of soil GHG in CC may be fundamentally different, as the rapid vegetation recovery after CC will lower the water table.

CRediT authorship contribution statement

Xuefei Li: Writing – original draft, Software, Methodology, Formal analysis, Conceptualization. **Tiina Markkanen:** Software, Methodology. **Mika Korkiakoski:** Resources, Investigation. **Annalea Lohila:** Resources, Investigation. **Antti Leppänen:** Software, Methodology. **Tuula Aalto:** Supervision, Conceptualization. **Mikko Peltoniemi:** Supervision, Resources. **Raisa Mäkipää:** Supervision, Resources, Conceptualization. **Thomas Kleinen:** Software, Methodology. **Maarit Raivonen:** Software, Methodology, Conceptualization.

Declaration of competing interest

The authors declare that they have no known competing financial interests or personal relationships that could have appeared to influence the work reported in this paper.

Data availability

Meteorological and environmental data measured at Lettosuo site are openly available through ICOS Carbon Portal (https://www.icos-cp.eu/observations/carbon-portal). Meteorological data measured at Jokioinen Ilmala, Salo Kiikala and Somero Salkola are openly available via Finnish Meteorological Institute open data service (https://en.ilmatieteenlaitos.fi/download-observations). Ecosystem flux data are available online (https://doi.org/10.1016/j.agrformet.2023.109361). Automatic CH4 chamber data are available online (https://doi.org/10.1016/j.agrformet.2020.108168). Manual CH4 and CO2 chamber data are available online (https://zenodo.org/records/3384791). Forest floor soil respiration data and water level data are available from this study through Zenodo (10.5281/zenodo.13347184). The JSBACH model source code can be obtained from the Max Planck Institute for Meteorology, where it is available for the scientific community under the MPI-M Sofware License Agreement (https://mpimet.mpg.de/en/research/modeling). The HIMMELI v200 source code is available through Zenodo (10.5281/zenodo.12532321). Further data can be obtained from the corresponding author.

Acknowledgments

This work was financially supported by the Strategic Research Council at the Research Council of Finland (STN-SOMPA, 312932 and 336573), Research Council of Finland (nos. 332953, 325169, 341752 and 341753), MMM Grant no. 4400T-2105 (TURNEE), EU-HORIZON ALFAWETLANDS (101056844), EU-H2020 VERIFY (776810), EU-HORIZON Eye-Clima (101081395), WetHorizons (Horizon Europe GAP-101056848) and the Ministry of Transport and Communications through the Integrated Carbon Observing System (ICOS) research. TK acknowledges support via the “PalMod” project, funded by the German Federal Ministry of Education and Research (BMBF), Grant No. 01LP1921A.

We thank K. Leppä for providing the meteorological forcing data to run JSBACH model and A. Putkinen for providing the CH_4 oxidation and production potentials from Lettosuo.

Appendix A. Supplementary data

Supplementary data to this article can be found online at https://doi.org/10.1016/j.scitotenv.2024.175257.

References

Aubinet, M., Vesala, T., Papale, D.E., 2012. Eddy Covariance: A Practical Guide to Measurement and Data Analysis. Springer Science & Business Media.
Böttcher, K., Markkanen, T., Thum, T., Aalto, T., Aurela, M., Reick, C.H., Kolari, P., Arslan, A.N., Pulliainen, J., 2016. Evaluating biosphere model estimates of the start of the vegetation active season in boreal forests by satellite observations. Remote Sens. 8 (7), 580 https://doi.org/10.3390/rs8070580.
Clymo, T.S., Turunen, J., Tolonen, K., 1998. Carbon accumulation in peatland. Oikos 81 (2), 368–388. https://doi.org/10.2307/3547057.
Comas, X., Slater, L., Reeve, A., 2008. Seasonal geophysical monitoring of biogenic gases in a northern peatland: implications for temporal and spatial variability in free phase gas production rates. J. Geophys. Res. Biogeosci. 113 https://doi.org/10.1029/2007jg000575.
Couwenberg, J., Thiele, A., Tanneberger, F., Augustin, J., Barisch, S., Dubovik, D., Liashchynskaya, N., Michaelis, D., Minke, M., Skuratovich, A., Joosten, H., 2011. Assessing greenhouse gas emissions from peatlands using vegetation as a proxy. Hydrobiologia 674 (1), 67–89. https://doi.org/10.1007/s10750-011-0729-x.
Curry, C.L., 2007. Modeling the soil consumption of atmospheric methane at the global scale. Glob. Biogeochem. Cycles 21 (4). https://doi.org/10.1029/2006GB002818.
De Vos, B., Cools, N., Ilvesniemi, H., Vesterdal, L., Vanguelova, E., Camicelli, S., 2015. Benchmark values for Forest soil carbon stocks in Europe: results from a large scale forest soil survey. Geoderma 251, 33–46. https://doi.org/10.1016/j.geoderma.2015.03.008.
Farquhar, G.D., Caemmerer, S.V., Berry, J.A., 1980. A biochemical-model of photosynthetic CO_2 assimilation in leaves of C-3 species. Planta 149 (1), 78–90. https://doi.org/10.1007/bf00386231.
Goll, D.S., Brovkin, V., Liski, J., Raddatz, T., Thum, T., Todd-Brown, K.E.O., 2015. Strong dependence of CO_2 emissions from anthropogenic land cover change on initial land cover and soil carbon parametrization. Glob. Biogeochem. Cycles 29 (9), 1511–1523. https://doi.org/10.1002/2014gb004988.
Günther, A., Barthelmes, A., Huth, V., Joosten, H., Jurasinski, G., Koebsch, F., Couwenberg, J., 2020. Prompt rewetting of drained peatlands reduces climate warming despite methane emissions. Nat. Commun. 11 (1) https://doi.org/10.1038/s41467-020-15499-z.
Huang, X., Silvennoinen, H., Kløve, B., Regina, K., Kandel, T.P., Piayda, A., Karki, S., Lærke, P.E., Höglind, M., 2021. Modelling CO_2 and CH_4 emissions from drained peatlands with grass cultivation by the BASGRA-BGC model. Sci. Total Environ. 765 https://doi.org/10.1016/j.scitotenv.2020.144385.
Jansson, P.E., 2012. Coupmodel: model use, calibration, and validation. Trans. ASABE 55 (4), 1335–1344. https://doi.org/10.13031/2013.42245.
Jungkunst, H.F., Fiedler, S., 2007. Latitudinal differentiated water table control of carbon dioxide, methane and nitrous oxide fluxes from hydromorphic soils: feedbacks to climate change. Glob. Chang. Biol. 13 (12), 2668–2683. https://doi.org/10.1111/j.1365-2486.2007.01459.x.

Kaiser, S., Goeckede, M., Castro-Morales, K., Knoblauch, C., Ekici, A., Kleinen, T., Zubrzycki, S., Sachs, T., Wille, C., Beer, C., 2017. Process-based modelling of the methane balance in periglacial landscapes (Jsbach-methane). Geosci. Model Dev. 10 (1), 333–358. https://doi.org/10.5194/gmd-10-333-2017.

Kasimir, A., He, H.X., Coria, J., Norden, A., 2018. Land use of drained peatlands: greenhouse gas fluxes, plant production, and economics. Glob. Chang. Biol. 24 (8), 3302–3316. https://doi.org/10.1111/gcb.13931.

Kasimir, A., He, H., Jansson, P.E., Lohila, A., Minkkinen, K., 2021. Mosses are important for soil carbon sequestration in forested peatlands. Front. Environ. Sci. 9, 680430 https://doi.org/10.3389/fenvs.2021.680430.

Kleinen, T., Brovkin, V., Schuldt, R.J., 2012. A dynamic model of wetland extent and peat accumulation: results for the Holocene. Biogeosciences 9 (1), 235–248. https://doi.org/10.5194/bg-9-235-2012.

Kleinen, T., Mikolajewicz, U., Brovkin, V., 2020. Terrestrial methane emissions from the Last Glacial Maximum to the preindustrial period. Clim. Past 16, 575–595. https://doi.org/10.5194/cp-16-575-2020.

Korkiakoski, M., Tuovinen, J.P., Aurela, M., Koskinen, M., Minkkinen, K., Ojanen, P., Penttilä, T., Rainne, J., Laurila, T., Lohila, A., 2017. Methane exchange at the peatland forest floor – automatic chamber system exposes the dynamics of small fluxes. Biogeosciences 14, 1947–1967. https://doi.org/10.5194/bg-14-1947-2017.

Korkiakoski, M., Tuovinen, J.P., Penttila, T., Sarkkola, S., Ojanen, P., Minkkinen, K., Rainne, J., Laurila, T., Lohila, A., 2019. Greenhouse gas and energy fluxes in a boreal peatland forest after CC. Biogeosciences 16 (19), 3703–3723. https://doi.org/10.5194/bg-16-3703-2019.

Korkiakoski, M., Ojanen, P., Penttila, T., Minkkinen, K., Sarkkola, S., Rainne, J., Laurila, T., Lohila, A., 2020. Impact of partial harvest on CH_4 and N_2O balances of a drained boreal peatland forest. Agric. For. Meteorol. 295, 108168 https://doi.org/10.1016/j.agrformet.2020.108168.

Korkiakoski, M., Ojanen, P., Tuovinen, J.P., Minkkinen, K., Nevalainen, O., Penttila, T., Aurela, M., Laurila, T., Lohila, A., 2023. Partial cutting of a boreal nutrient-rich peatland forest causes radically less short-term on-site CO_2 emissions than clear-cutting. Agric. For. Meteorol. 332 https://doi.org/10.1016/j.agrformet.2023.109361.

Koskinen, M., Minkkinen, K., Ojanen, P., Kamarainen, M., Laurila, T., Lohila, A., 2014. Measurements of CO_2 exchange with an automated chamber system throughout the year: challenges in measuring night-time respiration on porous peat soil. Biogeosciences 11 (2), 347–363. https://doi.org/10.5194/bg-11-347-2014.

Lai, D.Y.F., 2009. Methane dynamics in northern peatlands: a review. Pedosphere 19 (4), 409–421. https://doi.org/10.1016/S1002-0160(09)00003-4.

Laurila, T., Aurela, M., Hatakka, J., Hotanen, J.-P., Jauhiainen, J., Korkiakoski, M., Korpela, L., Koskinen, M., Laiho, R., Lehtonen, A., Leppä, K., Linkosalmi, M., Lohila, A., Minkkinen, K., Mäkelä, T., Mäkiranta, P., Nieminen, M., Ojanen, P., Peltoniemi, M., Penttilä, T., Rainne, J., Rautakoski, H., Saarinen, M., Salovaara, P., Sarkkola, S., Mäkipää, R., 2021. Set-up and instrumentation of the greenhouse gas measurements on experimental sites of continuous cover forestry. In: Natural Resources and Bioeconomy Studies. Natural Resources Institute Finland, p. 51.

Leppä, K., Korkiakoski, M., Nieminen, M., Laiho, R., Hotanen, J.-P., Kieloaho, A.-J., Korpela, L., Laurila, T., Lohila, A., Minkkinen, K., Mäkipää, R., Ojanen, P., Pearson, M., Penttila, T., Tuovinen, J.-P., Launiainen, S., 2020. Vegetation controls of water and energy balance of a drained peatland forest: responses to alternative harvesting practices. Agric. For. Meteorol. 295, 108198 https://doi.org/10.1016/j.agrformet.2020.108198.

Lloyd, J., Taylor, J.A., 1994. On the temperature-dependence of soil respiration. Funct. Ecol. 8 (3), 315–323. https://doi.org/10.2307/2389824.

Mäkelä, J., Knauer, J., Aurela, M., Black, A., Heimann, M., Kobayashi, H., Lohila, A., Mammarella, I., Margolis, H., Markkanen, T., Susiluoto, J., Thum, T., Viskari, T., Zaehle, S., Aalto, T., 2019. Parameter calibration and stomatal conductance formulation comparison for boreal forests with adaptive population importance sampler in the land surface model JSBACH. Geosci. Model Dev. 12 (9), 4075–4098. https://doi.org/10.5194/gmd-12-4075-2019.

Mäkipää, R., Abramoff, R., Adamczyk, B., Baldy, V., Biryol, C., Bosela, M., Casals, P., Yuste, J.C., Dondini, M., Filipek, S., Garcia-Pausas, J., Gros, R., Gomoryova, E., Hashimoto, S., Hassegawa, M., Immonen, P., Laiho, R., Li, H.H., Li, Q., Luyssaert, S., Menival, C., Mori, T., Naudts, K., Santonja, M., Smolander, A., Toriyama, J., Tupek, B., Ubeda, X., Verkerk, P.J., Lehtonen, A., 2023. How does management affect soil C sequestration and greenhouse gas fluxes in boreal and temperate forests? - a review. For. Ecol. Manag. 529 https://doi.org/10.1016/j.foreco.2022.120637.

Mäkiranta, P., Minkkinen, K., Hytonen, J., Laine, J., 2008. Factors causing temporal and spatial variation in heterotrophic and rhizospheric components of soil respiration in afforested organic soil croplands in Finland. Soil Biol. Biochem. 40 (7), 1592–1600. https://doi.org/10.1016/j.soilbio.2008.01.009.

Mäkiranta, P., Laiho, R., Fritze, H., Hytonen, J., Laine, J., Minkkinen, K., 2009. Indirect regulation of heterotrophic peat soil respiration by water level via microbial community structure and temperature sensitivity. Soil Biol. Biochem. 41, 695–703. https://doi.org/10.1016/j.soilbio.2009.01.004.

Mäkiranta, P., Riutta, T., Penttila, T., Minkkinen, K., 2010. Dynamics of net ecosystem CO_2 exchange and heterotrophic soil respiration following clearfelling in a drained peatland forest. Agric. For. Meteorol. 150 (12), 1585–1596. https://doi.org/10.1016/j.agrformet.2010.08.010.

Mamkin, V., Kurbatova, J., Avilov, V., Ivanov, D., Kuricheva, O., Varlagin, A., Yaseneva, I., Olchev, A., 2019. Energy and CO_2 exchange in an undisturbed spruce forest and clear-cut in the Southern Taiga. Agric. For. Meteorol. 265, 252–268. https://doi.org/10.1016/j.agrformet.2018.11.018.

Martikainen, P.J., Nykanen, H., Alm, J., Silvola, J., 1995. Change in fluxes of carbon-dioxide, methane and nitrous-oxide due to forest drainage of mire sites of different trophy. Plant Soil 168, 571–577. https://doi.org/10.1007/bf00029370.

Mayer, M., Prescott, C.E., Abaker, W.E.A., Augusto, L., Cecillon, L., Ferreira, G.W.D., James, J., Jandl, R., Katzensteiner, K., Laclau, J.P., Laganiere, J., Nouvellon, Y., Pare, D., Stanturf, J.A., Vanguelova, E.I., Vesterdal, L., 2020. Tamm review: influence of forest management activities on soil organic carbon stocks: a knowledge synthesis. For. Ecol. Manag. 466 https://doi.org/10.1016/j.foreco.2020.118127.

Melloh, R.A., Crill, P.M., 1996. Winter methane dynamics in a temperate peatland. Glob. Biogeochem. Cycles 10 (2), 247–254. https://doi.org/10.1029/96gb00365.

Minkkinen, K., Laine, J., 1998. Long-term effect of forest drainage on the peat carbon stores of pine mires in Finland. Can. J. For. Res. Rev. Can. Rech. For. 28 (9), 1267–1275. https://doi.org/10.1139/cjfr-28-9-1267.

Moore, T., Basiliko, N., 2006. Decomposition in boreal peatlands. In: Wieder, R.K., Vitt, D.H. (Eds.), Boreal Peatland Ecosystems, Ecological Studies (Analysis and Synthesis), vol 188. Springer, pp. 125–143. https://doi.org/10.1007/978-3-540-31913-9_7.

Murguia-Flores, F., Arndt, S., Ganesan, A.L., Murray-Tortarolo, G., Hornibrook, E.R.C., 2018. Soil Methanotrophy Model (MeMo v1.0): a process-based model to quantify global uptake of atmospheric methane by soil. Geosci. Model Dev. 11, 2009–2032. https://doi.org/10.5194/gmd-11-2009-2018.

Neubauer, S.C., Megonigal, J.P., 2015. Moving beyond global warming potentials to quantify the climatic role of ecosystems. Ecosystems 18 (6), 1000–1013. https://doi.org/10.1007/s10021-015-9879-4.

Ngao, J., Longdoz, B., Granier, A., Epron, D., 2007. Estimation of autotrophic and heterotrophic components of soil respiration by trenching is sensitive to corrections for root decomposition and changes in soil water content. Plant Soil 301 (1–2), 99–110. https://doi.org/10.1007/s11104-007-9425-z.

Nichols, J.E., Peteet, D.M., 2019. Rapid expansion of northern peatlands and doubled estimate of carbon storage. Nat. Geosci. 12 (11) https://doi.org/10.1038/s41561-019-0454-z.

Nieminen, M., Hokka, H., Laiho, R., Juutinen, A., Ahtikoski, A., Pearson, M., Kojola, S., Sarkkola, S., Launiainen, S., Valkonen, S., Penttila, T., Lohila, A., Saarinen, M., Haahti, K., Makipaa, R., Miettinen, J., Ollikainen, M., 2018. Could continuous cover forestry be an economically and environmentally feasible management option on drained boreal peatlands? For. Ecol. Manag. 424, 78–84. https://doi.org/10.1016/j.foreco.2018.04.046.

Nilsson, M., Öquist, M., 2009. Partitioning litter mass loss into carbon dioxide and methane in peatland ecosystems. Geoph. Monog. Series, Carbon Cycling in Northern Peatlands 184, 131–144. https://doi.org/10.1029/2008GM000819.

Ojanen, P., Minkkinen, K., 2019. The dependence of net soil CO_2 emissions on water table depth in boreal peatlands drained for forestry. Mires Peat 24, 27. https://doi.org/10.19189/MaP.2019.OMB.StA.1751.

Ojanen, P., Minkkinen, K., Alm, J., Penttila, T., 2010. Soil-atmosphere CO_2, CH_4 and N_2O fluxes in boreal forestry-drained peatlands. For. Ecol. Manag. 260 (3), 411–421. https://doi.org/10.1016/j.foreco.2010.04.036.

Ojanen, P., Minkkinen, K., Penttila, T., 2013. The current greenhouse gas impact of forestry-drained boreal peatlands. For. Ecol. Manag. 289, 201–208. https://doi.org/10.1016/j.foreco.2012.10.008.

Paavilainen, E., Päivänen, J., 1995. Peatland Forestry: Ecology and Principles. Springer, Berlin, Germany.

Päivänen, J., Hånell, B., 2012. Peatland Ecology and Forestry: A Sound Approach. (Vol. University of Helsinki Department of Forest Sciences Publications). University of Helsinki Department of Forest Sciences Publications.

Peltoniemi, M., Li, Q., Turunen, P., Tupek, B., Mäkiranta, P., Leppä, K., Müller, M., Rissanen, A.J., Laiho, R., Anttila, J., Jauhiainen, J., Koskinen, M., Lehtonen, A., Ojanen, P., Pihlatie, M., Sarkkola, S., Vainio, E., Mäkibää, R., 2023. Soil GHG dynamics after water level rise - impacts of selection harvesting in peatland forests. Sci. Total Environ. 901, 165421 https://doi.org/10.1016/j.scitotenv.2023.165421.

Petrescu, A.M.R., Qiu, C.J., McGrath, M.J., Peylin, P., Peters, G.P., Ciais, P., Thompson, R.L., Tsuruta, A., Brunner, D., Kuhnert, M., Matthews, B., Palmer, P.I., Tarasova, O., Regnier, P., Lauerwald, R., Bastviken, D., Hoglund-Isaksson, L., Winiwarter, W., Etiope, G., Aalto, T., Balsamo, G., Bastrikov, V., Berchet, A., Brockmann, P., Ciotoli, G., Conchedda, G., Crippa, M., Dentener, F., Zwaaftink, C.D. G., Guizzardi, D., Gnnther, D., Haussaire, J.M., Houweling, S., Janssens-Maenhout, G., Kouyate, M., Leip, A., LeppSnen, A., Lugato, E., Maisonnier, M., Manning, A.J., Markkanen, T., McNorton, J., Muntean, M., Oreggioni, G.D., Patra, P. K., Perugini, L., Pison, I., Raivonen, M.T., Saunois, M., Segers, A.J., Smith, P., Solazzo, E., Tian, H.Q., Tubiello, F.N., Vesala, T., van der Werf, G.R., Wilson, C., Zaehle, S., 2023. The consolidated European synthesis of CH_4 and N_2O emissions for the European Union and United Kingdom: 1990-2019. Earth Syst. Sci. Data 15 (3), 1197–1268. https://doi.org/10.5194/essd-15-1197-2023.

Pirinen, P., Simola, H., Aalto, J., Kaukoranta, J.-P., Karlsson, P., Ruuhela, R., 2012. Tilastoja Suomen Ilmastosta 1981–2010 (Climatological Statistics of Finland 1981–2010).

Pumpanen, J., Kulmala, L., Linden, A., Kolari, P., Nikinmaa, E., Hari, P., 2015. Seasonal dynamics of autotrophic respiration in boreal forest soil estimated by continuous chamber measurements. Boreal Environ. Res. 20 (5), 637–650.

Raivonen, M., Smolander, S., Backman, L., Susiluoto, J., Aalto, T., Markkanen, T., Makela, J., Rinne, J., Peltola, O., Aurela, M., Lohila, A., Tomasic, M., Li, X.F., Larmola, T., Juutinen, S., Tuittila, E.S., Heimann, M., Sevanto, S., Kleinen, T., Brovkin, V., Vesala, T., 2017. HIMMELI v1.0: HelsinkI Model of MEthane buiLd-up and emIssion for peatlands. Geosci. Model Dev. 10 (12), 4665–4691. https://doi.org/10.5194/gmd-10-4665-2017.

Reick, C.H., Gayler, V., Goll, D.S., Hagemann, S., Heidkamp, M., Nabel, J.E.M.S., Raddatz, T., Roeckner, E., Schnur, R., Wilkenskjeld, S., 2021. JSBACH 3 - the land component of the MPI Earth System Model: documentation of version 3.2. In: Berichte zur Erdsystemforschung, 240. https://doi.org/10.17617/2.3279802.

Riley, W.J., Subin, Z.M., Lawrence, D.M., Swenson, S.C., Torn, M.S., Meng, L., Mahowald, N.M., Hess, P., 2011. Barriers to predicting changes in global terrestrial methane fluxes: analyses using CLM4Me, a methane biogeochemistry model integrated in CESM. Biogeosciences 8 (7), 1925–1953. https://doi.org/10.5194/bg-8-1925-2011.

Rinne, J., Tuittila, E.S., Peltola, O., Li, X.F., Raivonen, M., Alekseychik, P., Haapanala, S., Pihlatie, M., Aurela, M., Mammarella, I., Vesala, T., 2018. Temporal variation of ecosystem scale methane emission from a boreal fen in relation to temperature, water table position, and carbon dioxide fluxes. Glob. Biogeochem. Cycles 32 (7), 1087–1106. https://doi.org/10.1029/2017gb005747.

Sarkkola, S., Hokka, H., Koivusalo, H., Nieminen, M., Ahti, E., Paivanen, J., Laine, J., 2010. Role of tree stand evapotranspiration in maintaining satisfactory drainage conditions in drained peatlands. Can. J. For. Res. Rev. Can. Rech. For. 40 (8), 1485–1496. https://doi.org/10.1139/x10-084.

Sarkkola, S., Nieminen, M., Koivusalo, H., Lauren, A., Ahti, E., Launiainen, S., Nikinmaa, E., Marttila, H., Laine, J., Hokka, H., 2013. Domination of growing-season evapotranspiration over runoff makes ditch network maintenance in mature peatland forests questionable. Mires Peat 11, 1–11. Article 02.

Shanin, V., Juutinen, A., Ahtikoski, A., Frolov, P., Chertov, O., Ramo, J., Lehtonen, A., Laiho, R., Makiranta, P., Nieminen, M., Lauren, A., Sarkkola, S., Penttila, T., Tupek, B., Makipaa, R., 2021. Simulation modelling of greenhouse gas balance in continuous-cover forestry of Norway spruce stands on nutrient-rich drained peatlands. For. Ecol. Manag. 496, 119479 https://doi.org/10.1016/j.foreco.2021.119479.

Stephen, K.D., Arah, J.R.M., Daulat, N., Clymo, R.S., 1998. Root-mediated gas transport in peat determined by Argon diffusion. Soil Biol. Biochem. 30, 501–508.

Tang, J., Zhuang, Q., Shannon, R.D., White, J.R., 2010. Quantifying wetland methane emissions with process-based models of different complexities. Biogeosciences 7 (11), 3817–3837. https://doi.org/10.5194/bg-7-3817-2010.

Tuomi, M., Thum, T., Jarvinen, H., Fronzek, S., Berg, B., Harmon, M., Trofymow, J.A., Sevanto, S., Liski, J., 2009. Leaf litter decomposition-estimates of global variability based on Yasso07 model. Ecol. Model. 220 (23), 3362–3371. https://doi.org/10.1016/j.ecolmodel.2009.05.016.

Turunen, J., 2008. Development of Finnish peatland area and carbon storage 1950-2000. Boreal Environ. Res. 13 (4), 319–334.

Tyystjärvi, V., Markkanen, T., Backman, L., Raivonen, M., Leppänen, A., Li, X., Ojanen, P., Minkkinen, K., Hautala, R., Peltoniemi, M., Anttila, J., Laiho, R., Lohila, A., Mäkipää, R., Aalto, T., 2024. Future methane fluxes of peatlands are controlled by management practices and fluctuations in hydrological conditions due to climatic variability. EGUsphere. https://doi.org/10.5194/egusphere-2023-3037 [preprint].

Waddington, J.M., Roulet, N.T., 2000. Carbon balance of a boreal patterned peatland. Glob. Chang. Biol. 6 (1), 87–97. https://doi.org/10.1046/j.1365-2486.2000.00283.x.

Walter, B.P., Heimann, M., 2000. A process-based, climate-sensitive model to derive methane emissions from natural wetlands: application to five wetland sites, sensitivity to model parameters, and climate. Glob. Biogeochem. Cycles 14 (3), 745–765. https://doi.org/10.1029/1999gb001204.

Wania, R., Ross, I., Prentice, I.C., 2010. Implementation and evaluation of a new methane model within a dynamic global vegetation model: LPJ-WHyMe v1.3.1. Geosci. Model Dev. 3 (2), 565–584. https://doi.org/10.5194/gmd-3-565-2010.

Yang, L., Niu, S.L., Tian, D.S., Zhang, C.Y., Liu, W.G., Yu, Z., Yan, T., Yang, W., Zhao, X. H., Wang, J.S., 2022. A global synthesis reveals increases in soil greenhouse gas emissions under forest thinning. Sci. Total Environ. 804 https://doi.org/10.1016/j.scitotenv.2021.150225.

Yu, Z.C., 2011. Holocene carbon flux histories of the world's peatlands: global carbon-cycle implications. Holocene 21 (5), 761–774. https://doi.org/10.1177/0959683610386982.

Zhang, X.Z., Guan, D.X., Li, W.B., Sun, D., Jin, C.J., Yuan, F.H., Wang, A.Z., Wu, J.B., 2018. The effects of forest thinning on soil carbon stocks and dynamics: a meta-analysis. For. Ecol. Manag. 429 (Dec 2018), 36–43. https://doi.org/10.1016/j.foreco.2018.06.027.